Golden artefacts, resin figurines, body adhesives and tomb sediments from the pre-Columbian burial site El Caño (Gran Coclé, Panamá): Tracing organic contents using molecular archaeometry

Joeri Kaal [a,b,*], María Martín Seijo [c], César Oliveira [d], Ewa Wagner-Wysiecka [e,f], Victoria E. McCoy [g], Mónica M. Solórzano Kraemer [h], Alexander Kerner [i], Philip Wenig [i], Carlos Mayo [j], Julia Mayo [j,k,l]

[a] *Instituto de Ciencias del Patrimonio (Incipit), Consejo Superior de Investigaciones Científicas (CSIC), Santiago de Compostela, Spain*
[b] *Pyrolyscience, Madrid, Spain*
[c] *GEPN-AAT, Grupo de Estudos para a Prehistoria do Noroeste Ibérico-Arqueoloxía, Antigüidade e Territorio (GI-1534), Universidade de Santiago de Compostela, Santiago de Compostela, Spain*
[d] *Departamento de Ciências e Técnicas do Património, Faculdade de Letras, Universidade do Porto, Porto, Portugal*
[e] *Gdansk University of Technology, Faculty of Chemistry, Narutowicza 11/12, 80-233, Gdańsk, Poland*
[f] *International Amber Association, Warzywnicza 1, 80-838, Gdańsk, Poland*
[g] *Department of Geosciences, University of Wisconsin, Milwaukee, 3209 N Maryland Ave, Milwaukee, WI, 53211, USA*
[h] *Forschungsinstitut und Naturmuseum Senckenberg, Senckenberganlage 25, 60325, Frankfurt am Main, Germany*
[i] *Lablicate GmbH, Martin-Luther-King-Platz 6, 20146, Hamburg, Germany*
[j] *Centro de Investigaciones Arqueológicas del Istmo, Fundación El Caño, El Dorado, Panama*
[k] *Dirección Nacional de Patrimonio Histórico, Panamá, Panama*

[l] *National Research System (SNI) of the National Secretariat for Science, Technology and Innovation (SENACYT), Panamá, Panama*

A B S T R A C T

This research aimed to determine the origin of organic residues from funerary contexts in the El Caño settlement (Gran Coclé area, Panamá, Central America) by means of multiple molecular probing techniques (GC-MS of organic solvent extracts and pyrolysis-GC-MS, THM-GC-MS and FTIR of solid samples). The samples include particles of precious resin figurines, fillings of golden objects, tomb sediments, plant exudates from extant plants (reference collection) and other reference materials (amber). The labdane diterpene fingerprints (eperuic, iso- ozic, copalic and kolavenic acids and derivatives) of the resin figurines, a resinous bead and several other samples, suggest that they were composed primarily of *Hymenaea* resin. Besides traditional interpretation ap-proaches (visual comparison of chromatograms and relative proportions data), we used a novel OpenChrom® application that resolves complex pyrolysis chromatograms by screening data from archaeological samples for marker products defined on the basis of a reference collection (*ChromIdent*). ChromIdent confirmed the *Hyme-naea* origin of many samples and also Burseraceae resin was identified in some samples, which is present as a minor ingredient in resin figurines (indicative of mixing practices) and as the dominant resin in tomb sediment that had been in contact with the corpses (indicating balsaming practices). The degree of polymerization of the *Hymenaea* resin was higher than for extant resin but diagenetic alteration (especially condensation of cyclic moieties) was much smaller than for amber, implying that the manufacturers used resin (or copal), not amber. These results were confirmed by FTIR, which allowed identification of non-fossil *Hymenaea* resin as the main constituent of one of the resin figurines. Several golden object infillings contained wax derivatives, probably beeswax, accompanied by various types of plant resin, which may well indicate the use of meliponines' cerumen for manufacturing (lost-wax casting). The findings highlight the potential of complementary molecular tech-niques to resolve questions on materials and manufacturing of archaeological artefacts, and the need for cross- comparison of molecular and ethnographic information in the study of archaeobotanical remains and the pro-cesses involved in their management.

Keywords: El Caño site   Funerary context   Trousseau   Analytical chemistry   Terpenoids

1. Introduction

In central Panama, hierarchical societies that controlled natural resources, external trade networks, craft production and large-scale agriculture emerged around AD 750–800 (Linares, 1977; Cooke, 2004; Cooke et al., 2003; Dickau, 2010). Their archaeological characterization has been based on funerary contexts from the centre of the country where large amounts of sumptuary goods have been unearthed (Lothrop, 1937; Hearne and Sharer, 1992; Mayo and Carles, 2015) as well as in small-scale settlements (Cooke, 1972; Mayo et al., 2007). Recent discoveries at El Caño (Coclé province, Panamá) have revealed its use as a necropolis with multiple and simultaneous burials (Mayo and Carles, 2015; Mayo Torné et al., 2016) similar to those identified in Sitio Conte at the beginning of the 20th century (Lothrop, 1934, 1937). Inside these large tombs, different episodes related to the complex burial rite have been identified, which involved the disposition of multiple individuals –up to more than forty in Tomb 7– to accompany the elite members in their afterlife (Mayo Torné et al., 2016). The high-ranking individuals in the tombs were accompanied by valuable objects such as pectorals, ear ornaments, pendants, belts and bracelets made of *tumbaga* or gold, as well as other objects made of resin, copper, stone and bone, and massive deposits of ceramics and other perishable goods (Mayo and Carles, 2015; Mayo Torné et al., 2016). The wealth of these tombs can be attributed to the non-state stratified society of the Neotropic chiefdoms, which developed a complex social, political and economical organization since AD 700 in the Parita Bay.

The use of resins in the burial rites identified in El Caño, as well as in Sitio Conte (Lothrop, 1934, 1937; Linares, 1977) was not restricted to their use as a raw material for crafting objects such as beads, pendants and other figurines (Mason, 1940; Hearne and Sharer, 1992), but also as incense to emit fragrant fumes in the *sahumerios* and for embalming practices (Cooke et al., 2003). The burning of resins was described in the written sources by Fernández de Oviedo (IX, XXX, 357), and has been attested archaeologically by the presence of incense vessels inside the tombs. It has been hypothesized that the corpse of the main individual buried in Tomb 2 was desiccated and shrouded using resins and textiles (Mayo and Carles, 2015), in a similar way as described for the Darien during the 16th century AD (Fernández de Oviedo, 1853: 155). Despite of the relevance of this kind of organic materials in the burial rites, few molecular analyses have been performed for their characterization, with the exception of resin figurines from Costa Rica dated to the period ranging from AD 700–1400 (Stone, 1963; Langenheim and Balser, 1975).

Especially since the "archaeological biomarker revolution" (Evershed, 2008), molecular fingerprinting of organic substances in archaeological objects is common practice. Methodology that is often employed are liquid and gas chromatographic analyses of organic solvent extracts (including total lipid extracts), in combination with mass spectrometry (LC-MS, GC-MS), and spectroscopic techniques such as Fourier-transform infrared spectroscopy (FTIR) and nuclear magnetic resonance (e.g. ^{13}C NMR) (Evershed, 1993; Ghisalberti and Godfrey, 1998; Evershed, 2008; Shillito et al., 2008; Colombini and Modugno, 2009; Mills and White, 2015). Less frequently, organic contents are released for GC-MS analysis using a rapid or instantaneous thermal pulse, such as pyrolysis-GC-MS (Py-GC-MS; e.g. Shedrinsky et al., 1989). Using pyrolytic approaches, not only volatiles but also macromolecular constituents can be analyzed on the molecular scale because pyrolysis breaks labile bonds creating GC-amenable products of biopolymers such as protein, lignin, polysaccharides and tannin, and polymerized resin. The heating can also be applied in the presence of reagents that promote hydrolysis and facilitate simultaneous derivatization, such as thermally assisted hydrolysis and methylation (THM-GC-MS; Challinor, 2001), sometimes referred to as thermochemolysis or Py(TMAH)-GC-MS.

In the present study, we applied FTIR, GC-MS, Py-GC-MS and THM-GC-MS to archaeological samples from El Caño. Special attention is given to a series of artefacts that are composed of natural resins (resin

figurines, beads) (Fig. 1), for which these methods have demonstrated potential (Chiavari and Prati, 2003; de la Cruz et al., 2005; Colombini et al., 2013; Mills and White, 2015; Łucejko et al., 2017; Traoré et al., 2018). For resinous objects, molecular characterization allows to identify the type of resin on the basis of the balance of mono-, sesqui-, di- and triterpenoids, and in many cases to identify the botanical source from specific structural features and/or identification of biomarkers on the level of genus or species (Shillito et al., 2008). Furthermore, the impact of thermal alteration on natural resins can be established from terpenoid condensation parameters which can be used to evaluate e.g. manufacturing processes (Evershed, 2008) and, in case of geologically modified resin, the type of amber deposits (Anderson and Winans, 1991; Ragazzi et al., 2003; Tappert et al., 2011; Seyfullah et al., 2015). The methods are also suitable for identification of non-resinous types of organic matter, which renders them suitable for analysis of organic matter in sediments and golden objects with unknown organic contents.

The accuracy in chemical identification of organic remains in archaeological samples, and in particular that of plant derivatives, relies heavily on how information from (1) studies on similar materials and methodology, including reference collections, and (2) ethnographical studies of the identified source candidates and use-related/taphonomical alterations, is managed. Molecular analyses rarely provide independent and conclusive evidence on human-plant interrelationships, but can often indicate broad origins which can be refined to specific sources and processing techniques by argumentation using non-analytical information (archaeological record and theory). Interpretation of chemical data without knowledge of the ethnographical symbolism of the materials used for the creation of the targeted objects can lead to unrealistic conclusions, and *vice versa* lack of evidence from chemical analyses can imply that contrasting hypotheses remain open to debate. Hence, a multidisciplinary approach is required.

The objective of the present study was to identify the organic matter in diverse samples from tombs in the El Caño burial site, and relate that information to raw material selection, artefact manufacturing and funerary practices.

2. Materials and methods

2.1. Archaeological site and samples

El Caño necropolis (Gran Coclé archaeological tradition) is located at 50 m.a.s.l. on the Pacific slope of Panama, in the alluvial plain of the Río Grande river, which flows from the Cordillera Central mountains to the Parita Bay (Fig. 2). The site is composed by (at least) a ceremonial area and a cemetery. The ceremonial area contains stone structures including a cobblestone pathway, two alignments of basalt columns and a group of 37 stone sculptures, two altars and two carved columns (Verril, 1972; Zelsman, 1959; Doyle, 1960; Cooke, 1976; Mayo and Mayo, 2013a, 2013b). The cemetery was organized according to status criteria in at least two sections (Fig. 2). Between 2008 and 2017, seven tombs built from wood and other plant-based materials in the elite section were excavated (Hervás Herrera, 2018; Martín-Seijo et al., 2016, 2018). The investigations provided information on funerary rituals and social organization of the complex societies in the region between cal. AD 750–1020 (Mayo Torné et al., 2016, Mayo et al., in press).

Twenty samples were recovered from stratigraphic units related to burials (Table 1). They were taken from artefacts of the mortuary ensembles and from surroundings of the skeletal remains in order to identify materials used in the shrouding process. The samples analyzed originate from four tombs of the elite section of the cemetery (Fig. 2), i.e. Tombs 1, 2, 4 and 7.

2.2. Reference collection (exudates from living plants)

Kaal et al. (2018) described the composition of the resins, gums and mucilages of the reference collection, consisting of 11 ethnographically

important botanical species from Central America (*Spondias mombin*, *Bursera tomentosa*, *B. simaruba*, *Tetragastris panamensis*, *Copaifera aromatica*, *Hymenaea courbaril*, *Albizia adinocephala*, *Albizia guachapele*, *Enterolobium cyclocarpum*, *Castilla elastica* and *Pachira quinata*). That paper briefly discussed the GC-MC, Py-GC-MS and THM-GC-MS data. Five of these species (*B. tomentosa*, *B. simaruba*, *H. courbaril*, *S. mombin* and *T. panamensis*) provided molecular fingerprints of terpenoid materials whereas the other samples contained gum exudates (polymeric carbohydrate, tannin and proteinaceous materials only recognized by Py-GC-MS and THM-GC-MS), with the exception of *C. elastica* which produced a clear signal of latex (i.e., polyisoprene rubber). Here, the molecular fingerprints of these exudates are used to identify constituents of the archaeological samples.

2.3. Other reference materials

Hymenaea-derived Colombian copal and a sample of Mexican amber from Totolapa, Chiapas, were analyzed using Py-GC-MS, THM-GC-MS and FTIR to determine the effects of diagenetic alteration on the molecular fingerprint of *Hymenaea* resins and compare those to the archaeological samples. We have made no attempt to distinguish different species of the *Hymenaea* genus for extant resins. Neither did we do so for amber, as it is known that identification of the botanical origin of amber on the species level is difficult (Lambert et al., 2014; McCoy et al., 2017). Mexican amber is thought to be produced by an extinct

species, possibly *H. mexicana* or *H. allendis* (Brown, 2002; Calvillo-Canadell et al., 2010). The botanical origin of the Colombian copal sample is constrained to *Hymenaea* based on chemical analyses and because *Hymenaea* species are the most common resiniferous trees in the area (Clifford et al., 1997; Lambert et al., 2012; McCoy et al., 2017).

2.4. Analytical

2.4.1. GC-MS

Approximately 5 mg was collected from the surface of each sample and then crushed to powder on an agate mortar, to maximize the contact area and improve the efficiency of extraction. The organic remains were extracted twice in mixtures of chloroform:methanol (v:v 2:1) in an ultrasonic device. The combined extracts were filtered with 0.2 μm PTFE syringe filters and dried under N_2 flow, redissolved in pyridine and derivatized with 99:1 *N*,*O*-bis(trimethylsilyl) trifluoroacetamide (BSTFA):trimethylchlorosilane (TMSCl). The chromatographic analyses were performed with a Thermo Scientific™ ISQ Single Quadrupole GC-MS system, operating in full scan mode with the following experimental conditions: a) 60 m × 0.25 mm × 0.25 μm HP-5MS column; b) helium as carrier gas with a constant flow of 1 mL min^{-1}; c) injection volume 1 μL; d) injector temperature 250 °C; e) electron ionization mode at 70 eV; f) GC-MS interface 290 °C; g) ion source 280 °C; h) scanned *m/z* 50 to 650. After a 2 min isothermal hold at 190 °C the oven was heated to 265 °C at 3 °C min^{-1}, then to 285 °C at 10 °C min^{-1} and to 300 °C at 0.5 °C min^{-1},
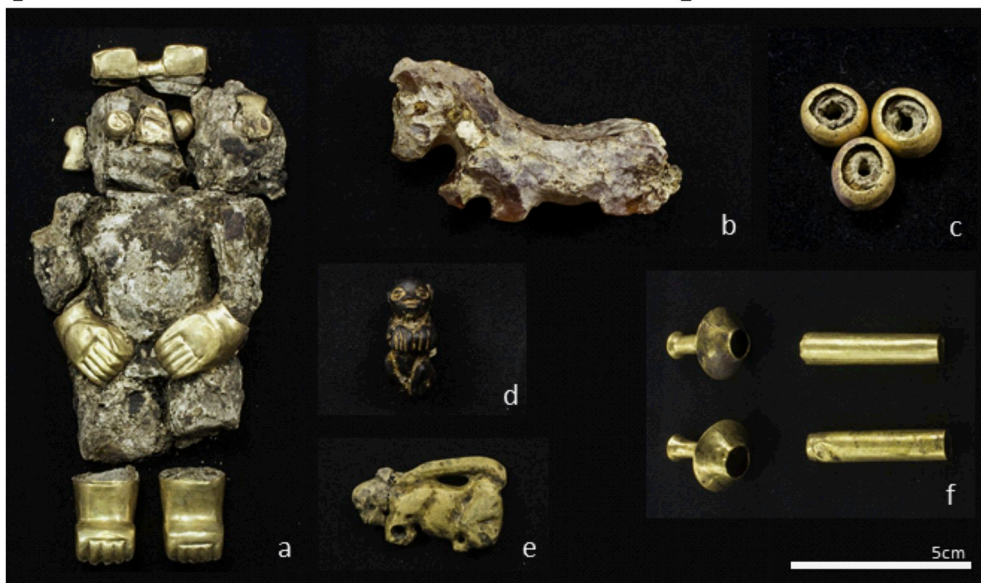
Fig. 1. Photographs of the tombs from which the studied samples were obtained and a selection of analyzed artefacts. 1) SU301 in tomb T7 (Photo: Miguel Ángel Hervás), 2) SU134 in tomb T2 (Photo: Julia Mayo), 3a) RESIN_02: anthropomorphic figurine with golden applications, 3b) RESIN_01: four-legged animal figurine; 3c) GOLD_06: tumbaga belt bead; 3d) RESIN_04: sloth figurine; 3e) RESIN_05: zoomorphic figurine and 3f) GOLD_05: tumbaga ear rod (Photos: Julia Mayo-3a, 3b, 3d and 3e; Carlos Gómez-3c and 3f).

and a final hold for 8 min (runtime 65 min). Compound identification was based on the NIST spectral library, available literature and analysis of fragmentation patterns.

2.4.2. Pyrolysis-GC-MS

Conventional analytical pyrolysis (Py-GC-MS) was performed using a Pyroprobe 5000 (CDS Analytical) coupled to a 5975 MSD system (Agilent Technologies). Solid sample material was placed in quartz-wool containing quartz tubes. The pyrolysis setpoint temperature was 650 °C (heating rate 10 °C ms^{-1}), maintained for 20 s. The pyrolysis interface, GC inlet and GC-MS interface were held at 325 °C. The GC operated in split mode (1:10). The oven was heated from 60 to 325 °C at 20 °C min^{-1} for most analysis, but for some samples additional runs using slower GC programs were used to improve chromatographic separation. Furthermore, there is a difference in retention times between the resin of *Copaifera aromatica* and the other resins (measured in different periods). The GC was equipped with a HP-5MS non-polar general purpose column. The single-quadrupole MS operated in electron impact mode (70 eV) and scanned in the 50–500 *m/z* range. Under these analytical conditions, the pyrolysis step not only releases macromolecular substances by breaking labile bonds but also evaporates volatiles. The resultant evaporation and pyrolysis products were transferred between the instruments using 1 ml min^{-1} helium flow. As the abundance of volatiles and pyrolyzable biopolymers in a sample were unknown, in many cases the analysis was repeated increasing the amount of sample (in case of low signal intensity) or decreasing it (in case of signal overload).

2.4.3. THM-GC-MS

The analytical conditions used for thermally assisted hydrolysis and

Table 1
List of samples with sample identifier (used in text), original inventory code, tomb number, stratigraphic unit (SU) and brief description.

Sample	Inventory code	Tomb	SU	Description
RESIN_01a	10248	T2	160	Four-legged animal figurine (bulk)
RESIN_01b	10248–01	T2	160	Four-legged animal figurine (interior)
RESIN_01c	10248–02	T2	160	Four-legged animal figurine (exterior)
RESIN_02	6685	T1	105	Anthropomorphic figurine with gold applications
RESIN_03	9285	T2	134	Anthropomorphic figurine with gold applications
RESIN_04	12014	T7	300	Sloth figurine
RESIN_05	11886	T7	300	Zoomorphic figurine
RESIN_06	12221	T7	301	Crocodile figurine
RESIN_07	11885	T7	301	Conic-shaped bead
GOLD_01	9321	T2	134	Tooth effigy pendant
GOLD_02	9574	T2	134	Embossed *tumbaga* pectoral disk
GOLD_03	7175	T2	106	*Tumbaga* ear rod
GOLD_04	11871	T4	391	*Tumbaga* bead
GOLD_05	12021	T7	301	*Tumbaga* ear rod
GOLD_06	11868	T7	301	Belt *tumbaga* bead
BODY_01	9832	T2	128	Resin residue
BODY_02	134-92-85	T2	134	Sediment associated to body 7
BODY_03	139	T4	391	Sediment in contact with a body
BODY_04	143	T4	391	Resin residue in contact with a body
BODY_05	144	T4	391	Resin in contact with a body

methylation were the same as for Py-GC-MS, with the exception of a 5 min solvent delay period at the start of the analysis. Prior to insertion of the pyrolysis probe into the pyrolysis interface, a droplet of 25%

Fig. 2. Location and context of the El Caño settlement and excavated tombs.

tetramethylammonium hydroxide (aqueous TMAH) was added to the sample-containing quartz tube. During the heating step, the hydrolyzable groups are hydrolyzed and simultaneously derivatized (methylated). This allows the detection of thermally labile groups such as carboxylic acids (as esters) and improves the chromatographic performance of otherwise polar groups.

2.4.4. FTIR

Three samples were submitted to the International Amber Association–Amber Laboratory (Gdańsk, Poland) for an independent identification of resin materials using FTIR, not providing information on context of the samples or hypotheses. The samples included the only archaeological sample that clearly corresponded to *Hymenaea* resin (on the basis of GC-MS, Py-GC-MS and THM-GC-MS) and for which sufficient material was available, i.e. figurine RESIN_02 (for which a larger piece of sample was extracted from the interior of the golden booth of the anthropomorph; Fig. 1). The other samples were Mexican amber (Totolapa, Chiapas) and Colombian copal. The FTIR spectra were recorded by Attenuated Total Reflectance (ATR) using a diamond crystal and measuring in the spectral range 4000-400 cm^{-1} (Nicolet iS10 FT-IR spectrometer). The resolution was 4 cm^{-1} and the number of scans both for background and sample was four. The spectra were subjected to advanced ATR correction and all analyzed spectra were baseline corrected, using standard spectrophotometer software.

2.5. Data evaluation

The GC-MS and THM-GC-MS data were interpreted qualitatively, i.e. on the basis of visual inspection of the chromatograms. For Py-GC-MS, the relative proportions of the main peaks (50–100 products) were calculated on the basis of peak areas (expressed as % of total quantified peak area, TQPA). This dataset was then used to compare samples and calculate proxies of resin maturity. For fingerprint recognition using ChromIdent, the original datafiles (*.D) are imported by OpenChrom and a series of data processing scripts were applied for retention time shifting (of the chromatogram of *Copaifera aromatica*), baseline correction, peak detection (first derivative) and peak integration (trapezoid peak shape fitting) (Wenig and Odermatt, 2010a, 2010b; Wenig, 2011). ChromIdent was used to calculate match qualities for extant resins and archaeological samples. Retention time deviations (up to 0.7 min), especially for the more abundant and polar products, have been corrected. The quality of the dataset was sufficient to use a minimum match score of 0.90 (Cosine Similarity Index, default is 0.75). This reduces the number of false-positive matches significantly. Especially for terpenoid analysis using electron ion mass spectrometry at 70 eV, this is useful to account for the typically intense ion fragmentation. For ChromIdent, the "training dataset" (terpenoid samples from the reference collection) included two replicates for Py-GC-MS.

Note that for GC-MS, Py-GC-MS and THM-GC-MS, it is not necessary, and in many cases impossible, to identify the exact molecular structure of a detected peak. Even though some of the peaks could be identified on the basis of mass fragmentometry, NIST libraries and comparison with literature, many others could only be identified on the basis of general structure (sesquiterpenoid, diterpenoid, triterpenoid), absence/presence of functional groups (-OH, –COOH), degree of aromaticity and sometimes acyclic alkyl side-chain configuration (vinyl-methyl, isopropyl, etc.). Despite of the recognition of such features, most of the compounds have multiple possible structures so that the identifications are tentative.

The interpretation of FTIR spectra was based on general rules of band assignment for functional organic group vibrations (Schrader, 1995; Larkin, 2011; Kiemle et al., 2019). The obtained spectra were compared with literature data (*vide infra*) and additional reference spectral material. The relative intensity of several specific bands was determined on the basis of peak height in the absorbance spectra.

3. Results and discussion

3.1. Reference collection (extant plants)

The samples of the Burseraceae family (*Bursera tomentosa*, *B. simaruba* and *Tetragastris panamensis*) share the feature of abundant pentacyclic triterpenoid signal including α-amyrin, β-amyrin and β-amyrinone (Kaal et al., 2018; Supplementary Information S1), accompanied with neooleananes, which confirms earlier studies (de la Cruz et al., 2005; Lucero-Gómez et al., 2014; Gigliarelli et al., 2015). The amyrins and related O-bearing pentacyclic triterpenoids with ursane and oleanane skeletal are polar high molecular weight compounds that are best observed (when using a non-polar GC column) after derivatization (GC-MS and THM-GC-MS), and quite poorly using Py-GC-MS. The main peaks that are characteristic of the Burseraceae triterpenoids have different relative intensities for the amyrin and related fragments, i.e. compounds producing m/z 218 > 190>189 (PT1), m/z 218 > 203>189 (PT2), m/z 218 > 189>203 (PT3) and m/z 69 > 393>218 (PT4) (Jacob et al., 2005; Supplementary Information S1). Their relative abundances are consistent (between the two techniques) and in the order of PT1>PT2>PT3 (*B. tomentosa*), PT4>PT3 (*B. simaruba*) and PT2>PT3 (*T. panamensis*), which allows distinguishing these species on the basis of pentacyclic triterpenoid composition. There are other sources of this kind of triterpenoid resins (Hernández-Vázquez et al., 2012), but the results suggest that a preliminary chemotaxonomic differentiation of relevant Burseraceae that are prolific of resin, is sustained. Furthermore, *T. panamensis* was prolific of sesquiterpenoids (Py-GC-MS and THM-GC-MS), in particular of C_5-hexa- and C_5-dihydronaphthalenes.

The resin exudates of the Fabaceae-Caesalpinoideae members *Hymenaea courbaril* and *Copaifera aromatica* are characterized by dominant sesquiterpenoids and labdatriene-type diterpenoids (bicyclic diterpenes with $C_{6:2}$ olefinic alkyl chain). In case of *Hymenaea*, these labdanes have an *enantio* configuration (Anderson, 1995), and its main labdane acids are iso-ozic acid, copalic acid, kolavenic acid and eperuic acid (e.g. Stankiewicz et al., 1998; Nogueira et al., 2001; Mills and White, 2015), which are detected as methyl and trimethylsilyl esters (ME, TMS) by THM-GC-MS (Doménech-Carbó et al., 2009) and GC-MS (McCoy et al., 2017), respectively. The labdane acid profiles using GC-MS and THM-GC-MS are similar, which confirms that the THM reaction does not cause drastic thermal degradation or isomerization (Anderson and Winans, 1991). Using THM-GC-MS, several compounds with M^+ 248 and 250 probably correspond to C_3- and C_4-hydronaphthoic acid MEs, i.e. labdane acids of which the exocyclic methylene chain was eliminated. This is the same formation pathway as suggested by Van den Berg (2003) for "communic acid pyrolysis products" (communic acid is a stereoisomer of ozic acid). Moreover, this effect was recognized by Clifford and Hatcher (1995) studying resinites in brown coal samples. Apparently, even hardened "fresh" resin had polymerized between sampling and analysis to an extent that the exocyclic alkyl side chain was affected, forming dealkylated labdane acid products (DLAP). The DLAP are detected using Py-GC-MS as well, more specifically C_4-hydronaphthoic acids (not detected as MEs: M^+ 234 for trihydro- and M^+ 236 for tetrahydronaphthoic acid) that are novel indicators of polymerized *Hymenaea* (*H. courbaril*, in this case) resin using Py-GC-MS (see below). For clarity, these are the underivatized analogues of the compounds reported by Van den Berg (2003) (compounds #70 and 71) and their mass spectral patterns are provided in Supplementary Information S2. The much less abundant underivatized analogue of C_3-tetrahydronaphthoic acid ME (M^+ 222) is presented for the sake of completeness, as well as tentative identifications of the TMS derivatives detected by GC-MS. Finally, some of the labdane acids were decarboxylated upon Py-GC-MS which explains why iso-ozic, eperuic and copalic/kovalenic acid are barely detectable in total ion current chromatograms of *Hymenaea* (Supplementary Information S1), giving rise to biformene and derivatives in the M^+ range 256–260.

The *Copaifera* sample is prolific of copalic acid and kovalenic acid

derivatives (and unidentified isomers thereof) after GC-MS and THM-GC-MS. Even though eperuic acid and perhaps some iso-ozic acid may be present, confusion with the *Hymenaea* fingerprint is impossible because, for the diterpenoid fraction, *Copaifera* has much less eperuic acid and much higher relative proportions of copalic and kovalenic acids than *Hymenaea* (Van den Berg, 2003; Supplementary Information S1). There are other significant differences: *Copaifera* produces large peaks for kaurenoic acid ME/TMS, kaurenoic acid ME/TMS and hardwickiic acid ME/TMS. These labdanoic acids survive pyrolytic decarboxylation to a significant extent, as shown by the presence of the dominant peak of copalic acid after Py-GC-MS. Decarboxylated copalic acid is also abundant, but this reaction does not result in the complete elimination of the exocyclic chain (which carries the carboxylic moiety in this case). Hence, the pyrolytic fragmentation of the labdane acids in *C. aromatica* does not allow for pathways that eliminate the exocyclic chain while pertaining the carboxylic moiety, and DLAP cannot be not formed. This difference can be related to the property of *Hymenaea* resin to polymerize very easily due to the position of the carboxylic group in iso-ozic acid at the C_4 and the *enantio* configuration (Mills and White, 2015).

In summary, the main differences in resin composition of the five resin species are the predominance of monoterpenoids and pentacyclic triterpenoids in the *Bursera* species, monoterpenoids and sesquiterpenoids in *Tetragastris panamensis* (and some amyrin), sesquiterpenoids and labdane acid diterpenoids (ozic, copalic, kolavenic, eperuic acid) in *Hymenaea courbaril*, and sesquiterpenoids and copalic/kolavenic acid-dominated labdane diterpenoids in *Copaifera aromatica*. The analyzed resins, at least in their fresh state, can be easily distinguished on the basis of their molecular composition, which encourages expanding the database in the future.

For the other species of the reference collection, i.e. the latex and gum fingerprints, GC-MS information was not obtained (weak or no signal due to poor solubilization) and the Py-GC-MS and THM-GC-MS fingerprints were tentatively recognized in only one archaeological sample, which is why these results are provided in Supplementary

Information S1.

3.2. Archaeological samples

3.2.1. Resin figurines

Selected chromatograms obtained by GC-MS (Fig. 3), Py-GC-MS (Fig. 4) and THM-GC-MS (Fig. 5) illustrate that the resin figures (RESIN_01–RESIN_06) and resinous bead (RESIN_07) share the feature of dominant sesquiterpenoid/labdane diterpenoid derivatives typical of *Hymenaea* resin. Using GC-MS and THM-GC-MS, these samples show large peaks for derivatized eperuic, copalic and kovalenic acids (Fig. 3, Table 2), along with some iso-ozic acid. For Py-GC-MS, the DLAP were identified in all these archaeological samples (Table 3; Supplementary Information S2). ChromIdent supports the identification as predominantly *Hymenaea*-like resin (i.e., not Burseraceae- or *Copaifera*-like): *Hymenaea* is the "best match" for all samples in terms of number of identified markers and overall match quality (Fig. 6; Table 4). Apart from the DLAP, compounds that were frequently marking *Hymenaea* in archaeological resin were C_3-benzene, C_3-naphthalene, C_4-napthalene and a compound giving rise to *m/z* 119, 133, 175 and 190 (probably decarboxylated DLAP). Furthermore, a minor peak that was often identified as a *Hymenaea* marker was tentatively identified as 2,5-dimethyl-1,3-hexadiene, which had passed unnoticed in chromatogram screenings, and might well correspond to the stripped exocyclic alkyl group of labdanoid compounds. The presence of the DLAP in *Hymenaea* resin but not in the most similar other resin specimen, i.e. that of *Copaifera aromatica* and the absence of hardwickiic acid derivatives (Van den Berg, 2003; Pinto et al., 2000) ascertained the *Hymenaea* rather than *Copaifera* origin.

From the zoomorph resin figure RESIN_01 three subsamples were taken. For the bulk sample (RESIN_01a), GC-MS did not provide a meaningful chromatogram due to poor solubility of the resin. RESIN_01b (Fig. 3) and RESIN_01c were prolific of labdane acids indicative of *Hymenaeae* resin. All samples showed traces of fatty acids, glycerol
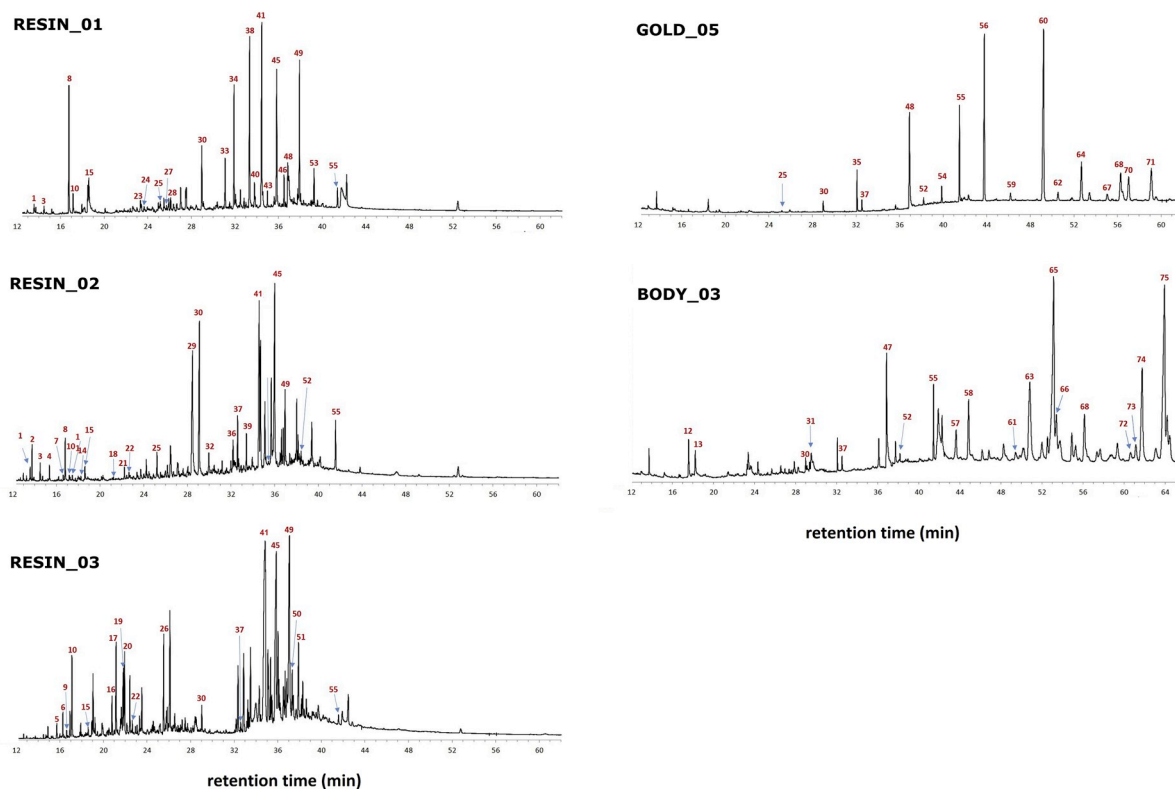
Fig. 3. Total ion current chromatograms obtained by GC-MS chromatograms (after TMS derivatization) of several examples of resin figurines (RESIN_01b, RESIN_02 and RESIN_03), golden object infilling (GOLD_05) and sediment associated with a corpse in tomb four (BODY_03). Peak labels refer to compounds listed in Table 3.
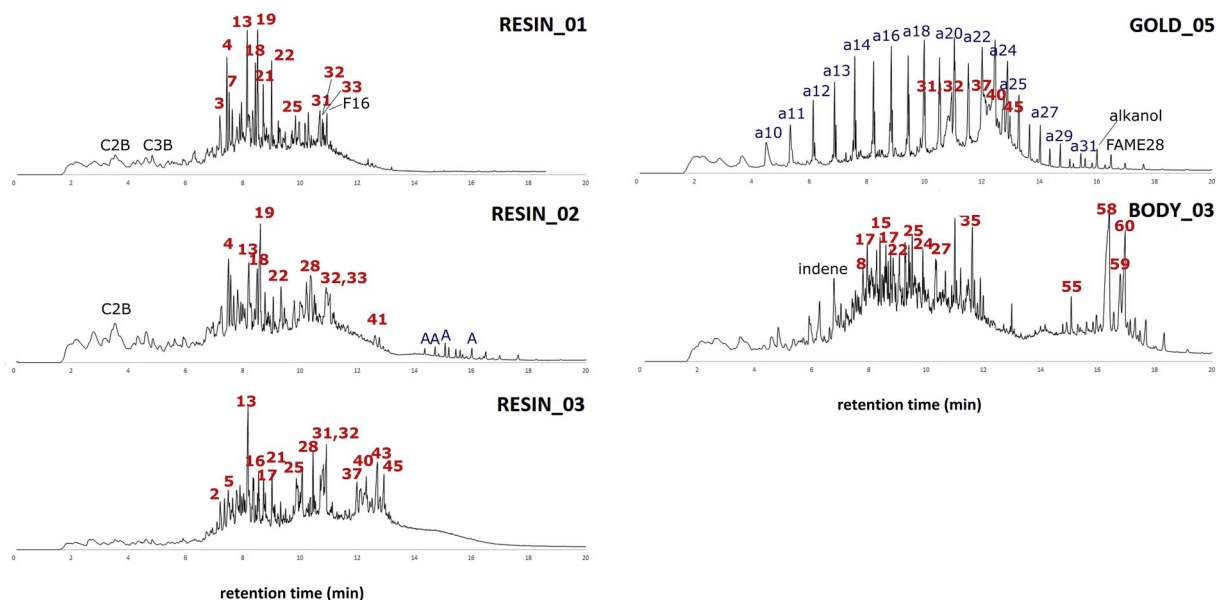
Fig. 4. Total ion current chromatograms obtained by Py-GC-MS chromatograms of resin figurines (RESIN_01b, RESIN_02 and RESIN_03), golden object infilling (GOLD_05) and sediment associated with a corpse in tomb four (BODY_03). Peak labels refer to terpenoid compounds listed in Table 4. Abbreviations of other products: C2B, C3B = dimethyl and trimethylbenzenes, F16 = palmitic acid, FAME28 = C_{28}-fatty acid methyl ester, A = alkane (unknown chain length), an = alkane/alkene doublet with chain length n.
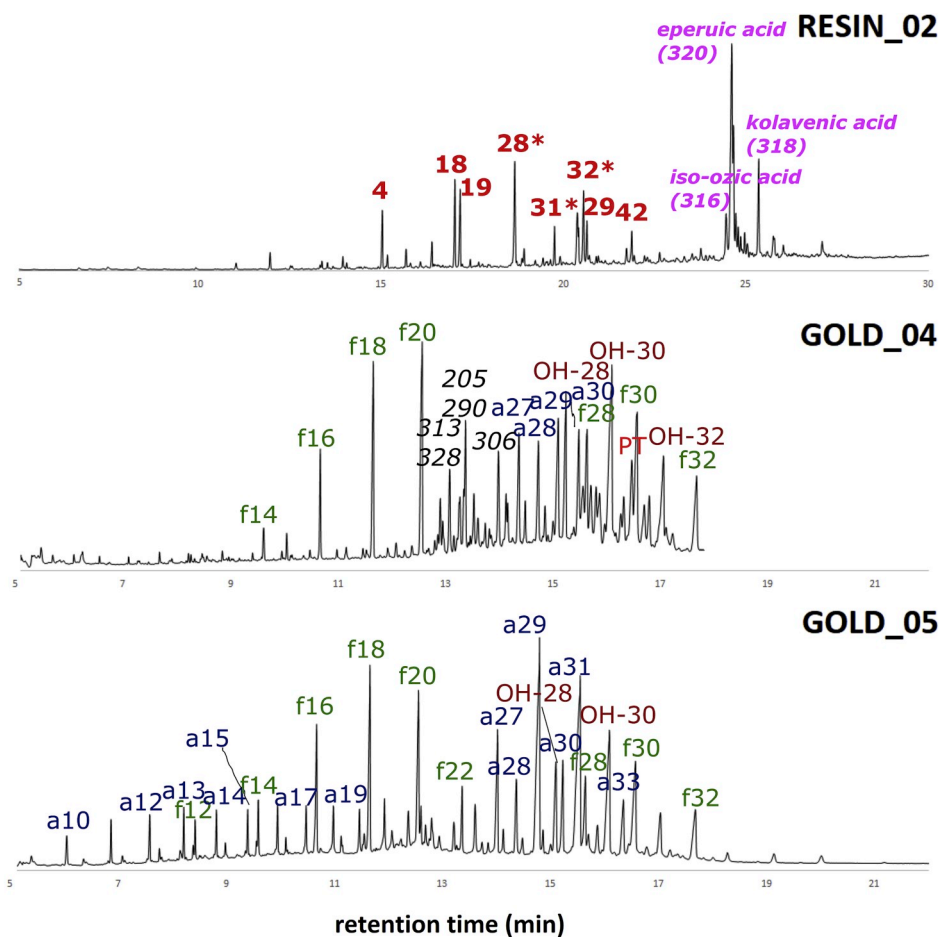
Fig. 5. Total ion current chromatograms obtained by THM-GC-MS chromatograms of resin figurine RESIN_02 and golden object infillings (GOLD_04 and GOLD_05). Peak labels in red refer to terpenoid compounds listed in Table 4 (same product as in Py-GC-MS). Abbreviations of other products: an = alkane with chain length n, fn = fatty acid methyl ester with chain length n, OH-n = alkanol (detected as methoxy) with chain length n, PT = pentacyclic triterpenoid. (For interpretation of the references to colour in this figure legend, the reader is referred to the Web version of this article.)

Table 2

List of main peaks in the GC-MS chromatograms (after TMS derivatization) of resin figurines (RESIN_01b, RESIN_02 and RESIN_03), golden object infilling (GOLD_05) and sediment associated with a corpse in tomb four (BODY_03). Labels 1–75 refer to peak labels in the example chromatograms (Fig. 3). PT1-PT3 refer to pentacyclic triterpenoids (see text).

label	RT (min)	Tentative identification
1	13.56	Octanoic acid
2	13.77	Glycerol
3	14.51	Butanedioic acid
4	15.36	Nonanoic acid
5	15.72	Neoclovene
6	16.27	Tricyclo[7.2.0.0(3,8)]undec-4-ene, 4,8,11,11-tetramethyl-
7	16.62	Longifolene
8	16.80	Gurjunene
9	16.93	Caryophyllene epoxide
10	17.15	Bergamotene
11	17.24	Decanoic acid
12	17.55	C_5-(10H)-naphthalene
13	18.19	C_5-(10H)-naphthalene
14	18.25	Hexanedioic acid
15	18.58	Bisabolene
16	20.79	11,11-dimethyl-8-methylenebicyclo[7.2.1]dodec-4-en-4-yl)oxy
17	21.17	$C_{15}H_{26}O$ isomer
18	21.22	Dodecanoic acid
19	21.83	Gurjunene epoxide
20	21.94	Muurolol
21	22.22	Suberic acid
22	22.64	$C_{15}H_{26}O$ isomer
23	23.32	Bisabolol
24	23.96	Eudesmol
25	25.15	Myristic acid
26	25.53	$C_{15}H_{26}O$ isomer
27	25.72	Eudesmol
28	26.10	$C_{15}H_{24}O$ isomer
29	28.48	C_2-dibenzothiophene
30	28.96	Palmitic acid
31	29.51	Cycloisolongifolene
32	29.96	Oleanitrile
33	31.11	Epimanool
34	31.92	Kaurene/biformene
35	32.09	4,4-Dimethyl-N-(2-phenylethyl)androst-2-en-17-amine
36	32.18	9-octadecenoic acid
37	32.51	Stearic acid
38	33.35	Ozic/communic acid
39	33.41	Ozic/communic acid
40	33.79	Kaurene/biformene
41	34.47	Eperuic acid
42	34.58	5-(7a-Isopropenyl-4,5-dimethyl-octahydroinden-4-yl)-3-methyl-pent-2-en-1-ol
43	34.99	Eperuic acid isomer
44	35.69	Oleamide
45	35.86	Copalic acid
46	36.51	Isolongifolol
47	36.85	24-norursa-3,12-diene
48	36.91	13-Docosenenitrile
49	36.95	Kolavenic acid
50	37.33	Kolavenic acid isomer
51	37.91	Kolavenic acid isomer
52	38.21	Monopalmitin
53	39.26	Ozic/communic acid isomer
54	39.87	Alkane
55	41.44	Monostearin
56	43.81	Alkane
57	43.83	Amyrin (PT1)
58	44.84	Amyrin (PT1)
59	46.19	Alkane
60	49.22	Alkane
61	49.43	Amyrone
62	50.54	Octacosanol (C_{28} alkanol)
63	52.00	Amyrin (PT2)
64	52.69	Alkane
65	53.14	Amyrin (PT3)
66	53.39	Lupeol
67	55.06	Amyrin (PT1)
68	56.13	Amyrin (PT1)

Table 2 (*continued*)

label	RT (min)	Tentative identification
69	56.30	Amyrin
70	57.02	Alkane
71	59.12	Triacontanol (C_{30} alkanol)
72	60.65	Amyrin (PT2)
73	61.16	Germanicol
74	61.76	Amyrin (PT2)
75	63.93	Amyrin (PT3)

and oleanitrile/oleamide, indicative of degraded lipids, probably of plant origin, but here contamination from the soil/tomb environment cannot be ruled out as a source. The relative intensity of these lipids decreases with signal intensity and thus resin availability/solubility. The GC-MS chromatograms of RESIN_01c contained traces of pentacyclic triterpenoids (e.g. α-amyrin and α-amyrone) which indicates the presence of burseraceous resin. Using Py-GC-MS, the signal of the *Hymenaea* resin overshadows that of any lipidic ingredient (Fig. 4), indicating that the pyrolysis step enhances the visibility of the resin structures probably by releasing polymerized moieties. The Py-GC-MS chromatograms of the three subsamples were almost identical, dominated by sesqui- and diterpenoids including DLAP. ChromIdent shows the presence of 15–20 *Hymenaea* markers including DLAP (Table 4). Some peaks were labelled as markers of *Copaifera*, including C_2-(2H)-naphthalene. For marker identifications of minor products, it is important to realize that ChromIdent scans for markers in the dataset of the reference collection using the total ion current, which implies that compounds with low abundance might not be included by the peak detector in one sample giving rise to an inadequate marker for another sample. This is especially cumbersome in fast-cycling GC-temperature programs such as the ones used here. Hence, for each "marker", its suitability was checked. Indeed, the C_2-(2H)-naphthalene was identified in the partial ion chromatogram of its main fragments m/z 143 and 158 of *Hymeanaea courbaril*, and presence of *Copaifera*-like resin was therefore deemed unlikely. Analogously, detection of *Hymenaea* markers DLAP, $C_{4:1}$-(4H)-naphthalene or 2,5-dimethyl-1,3-hexadiene was considered a much stronger indication of *Hymenaea*-like resin than presence of "markers" C_3-benzene, C_2-indene or C_3-naphthalene.

Sample RESIN_02 produced a GC-MS chromatogram with large peaks for derivatized labdane acids and some sesquiterpenoids, accompanied with fatty acids in the chain length range of C_{10} to C_{18}, glycerols of C_{16} and C_{18} fatty acids (glycerol palmitate/stearate), alkanes and oleanitrile, indicative of degraded vegetable fats in a matrix of *Hymenaea* resin (Fig. 3). Using Py-GC-MS the signal of the resin is again dominant (Fig. 4). For this sample THM-GC-MS could also be recorded, and showed large peaks for (1) sesquiterpenoids, (2) DLAP, (3) alkylnaphthalenes (due to polymerization/defunctionalization/condensation; Clifford and Hatcher, 1995; McCoy et al., 2017) and (4) labdane acids including iso-ozic, eperuic and copalic acid MEs (but not hardwickiic) (Fig. 5). The identification of *Hymenaea* resin was further confirmed by independent and blind analysis by FTIR (see section 3.4) and a good match with ChromIdent (Table 4).

Analysis of RESIN_03 by GC-MS gives strong signals of eperuic, copalic and kolavenic acids, in addition to many sesquiterpene derivatives (Fig. 3). The Py-GC-MS fingerprint shows the labdane diterpenoid structures observed in the other samples composed of *Hymenaea* resin (Fig. 4). In addition, RESIN_03 produced a series of unidentified compounds with base peak m/z 191 (M^+ 304 and 306), including an unidentified product with mass spectral pattern of m/z 136, 80 and 191. These compounds were also detected in sample GOLD_05 from the interior of a tubular earring (see below), but not in any of the samples from the reference collection. The lack of reference material to match the unidentified resin illustrates that the usefulness of ChromIdent depends on the size of the reference collection database.

Samples RESIN_04, RESIN_05, RESIN_06 and RESIN_07 did not

List of main peaks or terpenoid products (thus, alkanes, fatty acids and other non-terpenoid products are omitted) in the Py-GC-MS chromatograms. Relative proportions of the products in each archaeological sample (R = resin samples, G = infillings of golden objects, B = body adhesives/tomb sediments) are provided as the % of total quantified peak area (TQPA). Labels 1–60 refer to peak labels in the example chromatograms (Fig. 4). N.d. = not determined.

label	RT (min)	m/z	m/z	tentative identification	R01a	R01b	R01c	R02	R03	R04	R05	R06	R07	G06	G04	G05	B03	B03	B04	B05
1	7.013	161,176	161,176	$C_{3,1}$-(4H)-naphthalene	2.9	6.0	2.0	4.7	1.2	1.2	4.1	2.2	2.9	0.3	0.5	0.1	0.4	1.0	0.4	0.0
2	7.196	105,161,176	105,161,176	$C_{3,1}$-(4H)-naphthalene	3.9	6.9	2.5	3.3	2.4	1.4	3.6	2.6	2.8	3.9	0.7	0.1	0.8	0.6	0.5	0.1
3	7.222	160,145	160,145	C_2-(4H)-naphthalene	n.d.	8.0	3.2	5.3	0.4	1.7	6.0	3.2	5.0	0.2	0.8	0.2	1.0	0.7	0.6	0.4
4	7.440	177,192	177,192	C_4-(4H)-naphthalene	4.1	2.3	3.8	5.7	2.7	5.3	7.9	6.5	7.9	0.8	0.5	0.2	0.0	0.0	0.0	0.0
5	7.445	159,174	159,174	C_3-(4H)-naphthalene	4.8	0.0	0.0	0.0	0.0	0.0	0.0	0.0	0.0	2.2	4.9	0.7	0.4	1.5	1.2	0.7
6	7.497	191,204	191,204	unidentified compound	0.0	4.8	1.8	2.2	0.3	1.2	2.9	2.0	2.7	0.6	1.2	0.3	1.0	0.4	0.4	0.1
7	7.523	109 (119,177,192)	109 (119,177,192)	$C_{4,1}$-(6H)-naphthalene	1.9	7.8	4.6	7.4	3.0	4.1	6.7	4.9	7.0	3.0	7.2	0.8	8.6	7.1	3.3	0.9
8	7.637	143,158 (128)	143,158 (128)	C_2-(2H)-naphthalene	7.6	0.0	0.0	0.0	0.0	0.0	0.0	0.0	0.0	0.6	0.0	0.8	1.0	2.7	2.2	1.2
9	7.751	121,189,204	121,189,204	unidentified compound	0.0	3.4	0.0	3.7	2.1	0.5	2.1	1.2	1.1	2.1	6.7	0.1	0.1	0.4	0.2	0.1
10	7.881	161,176	161,176	$C_{3,1}$-(4H)-naphthalene	2.7	1.9	1.2	4.5	2.0	9.1	4.6	4.6	5.0	0.2	0.3	0.5	10.3	5.0	3.0	1.1
11	7.953	156,141	156,141	C_2-naphthalene	6.7	0.0	3.5	0.0	0.0	0.0	0.0	0.0	0.0	4.9	11.2	0.0	0.0	1.1	4.1	0.0
12	8.026	165,193,208 (109)	165,193,208 (109)	unidentified compound	0.0	11.7	0.0	5.8	8.4	0.9	5.6	4.1	2.9	0.7	1.1	0.3	0.0	0.0	0.0	0.2
13	8.151	119,105 (175,190)	119,105 (175,190)	$C_{4,1}$-(4H)-naphthalene	7.2	0.0	3.2	0.0	0.0	0.0	0.0	0.0	0.0	0.0	0.0	0.0	0.0	0.0	4.0	0.3
14	8.229	165,193,208	165,193,208	unidentified compound	0.0	0.0	0.0	0.0	0.0	0.0	0.0	0.0	0.0	0.8	0.5	0.3	0.0	0.0	0.0	0.2
15	8.343	145 (208)	145 (208)	unidentified compound	0.0	4.6	0.0	3.5	3.5	1.9	2.9	3.0	3.8	1.5	0.6	0.3	8.1	5.6	5.9	0.6
16	8.348	159,174	159,174	C_3-(4H)-naphthalene	5.2	2.2	2.7	1.7	3.6	1.6	2.9	2.2	0.9	1.1	2.4	0.5	4.7	5.6	3.6	0.2
17	8.390	173,188	173,188	C_4-(4H)-naphthalene	2.9	15.5	1.8	8.2	0.5	1.6	9.9	9.2	10.7	0.5	1.3	0.4	4.1	3.2	1.8	1.0
18	8.441	95,191,206	95,191,206	C_5-(8H)-naphthalene	5.5	8.0	5.1	6.3	0.9	1.6	10.4	7.6	8.9	0.7	1.5	0.3	0.0	0.0	0.0	0.0
19	8.514	119,105 (189,204)	119,105 (189,204)	$C_{5,1}$-(8H)-naphthalene	4.9	1.1	4.4	3.0	5.2	2.2	7.3	7.7	7.8	1.2	1.0	0.9	7.2	9.2	4.6	0.3
20	8.550	173,188	173,188	C_4-(4H)-naphthalene	5.5	3.9	3.9	5.1	4.7	2.6	5.8	5.2	4.6	0.8	0.4	0.2	2.3	3.2	0.9	0.2
21	8.716	157,172 (142)	157,172 (142)	C_5-(2H)-naphthalene	8.2	2.7	3.8	5.9	6.0	10.3	5.7	8.9	9.4	4.7	6.7	1.1	4.6	5.5	0.9	0.6
22	9.007	155,170	155,170	C_5-naphthalene	12.8	0.4	7.0	0.3	0.3	1.8	1.5	1.9	1.0	1.4	0.2	0.2	5.8	5.9	3.9	0.9
23	9.214	187,202	187,202	C_5-(4H)-naphthalene	0.8	0.0	0.8	0.0	0.0	0.0	0.0	0.0	0.0	0.0	0.0	0.0	4.0	4.4	5.4	0.1
24	9.386	108,216	108,216	unidentified compound	0.0	0.2	0.0	0.7	3.0	3.1	1.4	2.4	1.4	3.3	1.0	1.3	6.7	10.0	3.6	0.5
25	9.874	169,184	169,184	C_4-naphthalene	1.6	1.2	2.0	0.9	0.6	0.3	0.3	0.4	0.4	0.0	0.0	0.2	0.0	0.0	0.0	0.0
26	9.967	222 (161,177,207)	222 (161,177,207)	unsaturated C_5-naphthoic acid (VDB69)[a]	0.4	0.2	1.0	1.2	0.7	0.5	0.3	0.5	0.4	0.1	0.1	0.2	0.0	0.0	0.0	0.0
27	9.999	183,198	183,198	C_5-naphthalene	n.d	1.0	0.0	0.1	0.0	0.4	0.2	0.4	0.4	0.0	0.0	0.0	0.0	0.0	0.0	0.0
28	10.185	222 (161,177,207)	222 (161,177,207)	unsaturated C_5-naphthoic acid (VDB69)[a]	0.4	1.5	1.1	1.2	0.1	0.4	0.4	0.3	0.5	0.1	0.0	0.0	0.0	0.0	0.0	0.0
29	10.211	220 (97,135)	220 (97,135)	unsaturated C_5-naphthoic acid	0.1	0.6	0.1	0.1	0.0	0.4	0.2	0.4	0.5	0.0	0.0	0.0	0.0	0.0	0.0	0.0
30	10.309	220 (91,119)	220 (91,119)	unsaturated C_5-naphthoic acid	0.3	0.7	0.6	0.8	0.1	0.4	0.4	0.3	0.4	0.0	0.6	0.0	0.0	0.0	0.0	0.0
31	10.693	119,175,221 (236)	119,175,221 (236)	unsaturated C_4-naphthoic acid (VDB71)[a]	5.9	2.1	24.5	9.3	11.0	15.1	2.7	5.9	4.0	0.0	0.0	17.6	0.0	0.0	0.0	0.0
32	10.781	133,173,234	133,173,234	unsaturated C_4-naphthoic acid (VDB70)[a]	1.1	0.5	5.5	2.8	4.1	3.8	1.0	1.8	1.7	0.0	0.0	13.3	0.0	0.0	0.0	0.0
33	10.823	145,227,242	145,227,242	unidentified compound	1.4	1.9	2.7	2.4	1.0	2.3	3.4	3.3	2.8	0.0	0.0	0.0	0.4	0.0	0.2	0.1
34	11.357	215,230	215,230	unidentified compound	0.0	0.0	0.0	0.6	0.0	2.0	0.0	0.0	0.4	0.0	0.0	0.0	0.0	5.4	12.1	12.1
35	11.539	224,209	224,209	unidentified compound	0.0	0.0	0.0	0.0	0.0	0.0	0.0	0.0	0.0	0.0	0.0	0.0	8.4	11.3	7.7	5.7
36	11.549	206	206	unidentified compound	0.3	0.0	2.5	1.4	1.5	8.2	0.0	2.8	2.5	1.4	2.5	1.2	10.1	2.7	0.0	5.5
37	11.990	191	191	unidentified compound	0.0	0.0	0.5	0.3	6.9	0.3	0.0	0.2	0.1	0.0	14.1	16.5	0.0	0.0	0.0	5.0
38	12.016	241,256	241,256	unidentified compound	0.0	0.0	0.3	0.2	0.1	1.0	0.1	0.7	0.5	0.0	0.2	0.4	0.0	0.0	0.0	7.2
39	12.115	191	191	unidentified compound	0.0	0.0	0.3	0.1	6.2	0.3	0.0	0.1	0.0	0.0	0.0	0.0	0.3	0.2	0.0	3.5
40	12.307	136,80 (191)	136,80 (191)	unidentified compound	0.0	0.0	0.0	0.1	6.9	2.0	0.0	0.0	0.0	0.0	0.0	19.1	0.0	0.0	0.0	26.6
41	12.499	95,137 (291,306)	95,137 (291,306)	unidentified compound	0.2	0.0	2.0	1.1	4.5	0.0	0.0	0.8	0.0	0.0	0.0	16.7	0.0	0.0	0.0	0.1
42	12.660	257,272	257,272	enantio-biformene	0.2	0.0	0.4	0.6	1.3	3.9	0.0	1.5	0.4	0.0	0.0	0.0	0.0	0.0	0.0	11.1
43	12.712	191 (263,291,306)	191 (263,291,306)	unidentified compound	0.1	0.0	0.6	0.6	3.8	0.8	0.0	0.7	0.1	0.2	0.8	3.8	0.0	0.0	0.0	0.0
44	12.857	313,328 (203,218)	313,328 (203,218)	unidentified compound	0.0	0.0	0.1	0.2	0.0	0.1	0.0	0.0	0.0	0.8	0.1	0.0	0.0	0.0	0.0	7.9
45	12.935	191 (263,291,306)	191 (263,291,306)	unidentified compound	0.0	0.0	0.1	0.2	1.3	0.3	0.0	0.1	0.4	0.4	0.3	0.8	0.0	0.0	0.0	0.0
46	12.971	313,328	313,328	unidentified compound	0.0	0.0	0.1	0.0	0.0	0.2	0.0	0.0	0.0	4.2	6.9	0.1	0.1	0.1	0.0	11.1
47	13.090	218,203 (313,328)	218,203 (313,328)	unidentified compound	0.0	0.0	0.1	0.0	0.2	0.2	0.0	0.0	0.0	1.3	4.5	0.0	0.0	0.2	0.0	18.7
48	13.142	205,290 (313,328)	205,290 (313,328)	unidentified compound	0.0	0.0	0.0	0.0	0.0	0.2	0.0	0.0	0.0	5.1	12.3	0.1	1.0	0.1	0.2	5.7
49	13.422	207,292	207,292	unidentified compound	0.0	0.0	0.0	0.0	0.1	0.2	0.0	0.1	0.0	0.2	14.1	0.1	2.4	0.1	0.4	5.5
50	13.713	325,340	325,340	unidentified compound	0.0	0.0	0.0	0.0	0.1	0.2	0.0	0.2	0.1	0.2	0.2	0.0	0.0	0.2	0.0	5.0
51	13.978	232 (306,342)	232 (306,342)	unidentified compound	0.0	0.0	0.1	0.0	0.0	0.1	0.0	0.3	0.1	0.3	0.1	0.0	0.3	0.2	0.0	7.2
52	13.998	223,306	223,306	unidentified compound	0.0	0.0	0.0	0.0	0.0	0.0	0.0	0.0	0.0	3.9	2.6	0.0	0.0	0.1	0.0	3.5
53	14.170	232 (327,342)	232 (327,342)	unidentified compound	0.1	0.0	0.0	0.1	1.1	1.3	0.0	1.0	0.0	1.0	1.3	0.0	1.1	0.3	0.0	26.6
54	14.896	365 (393,408)	365 (393,408)	A-Neooleana-3(5),12-diene	0.0	0.0	0.0	0.0	0.0	0.3	0.0	0.1	0.0	0.8	0.1	0.0	1.5	0.6	4.2	0.1
55	15.057	365 (393,408)	365 (393,408)	A-Neooleana-3(5),12-diene	0.0	0.0	0.0	0.1	0.0	0.5	0.0	0.2	0.0	2.3	0.1	0.0	4.3	1.5	12.0	0.1
56	15.493	218,203,189 (408)	218,203,189 (408)	amyrin product (PT2)	0.0	0.0	0.1	0.1	0.0	0.7	0.0	0.3	0.1	6.6	0.1	0.0	1.8	0.2	3.4	0.0
57	15.700	218,189,203 (408)	218,189,203 (408)	amyrin product (PT1)	0.1	0.0	0.0	0.4	0.0	0.9	0.0	0.6	0.1	31.0	0.3	0.1	5.3	0.7	9.3	0.0
58	16.323	342,242	342,242	unidentified compound	n.d.	0.0	0.1	0.0	0.0	0.0	0.0	0.0	0.0	0.0	0.0	0.0	0.0	0.0	0.0	0.0
59	16.780	356,273	356,273	unidentified compound	n.d.	0.0	0.0	0.0	0.0	0.0	0.0	0.0	0.0	0.0	0.0	0.0	0.0	0.0	0.0	0.0
60	16.946	356,273	356,273	unidentified compound	n.d.	0.0	0.0	0.0	0.0	0.0	0.0	0.0	0.0	0.0	0.0	0.0	0.0	0.0	0.0	0.0

[a] Peak code for the terpenoid mass spectral database (Atlas) of Van den Berg (2003).
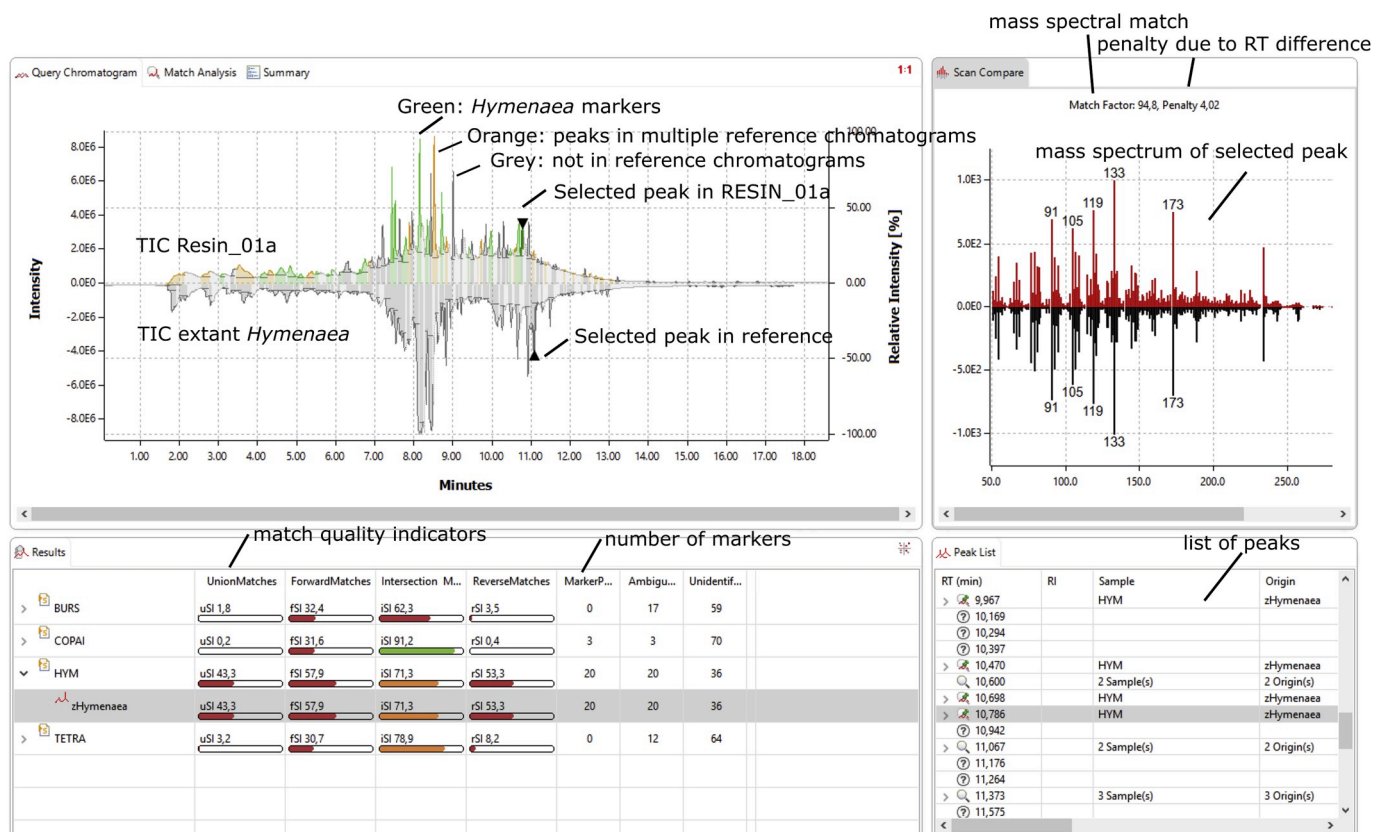
9

Fig. 6. Example of ChromIdent results for resin figurine sample RESIN_01a.

provide meaningful chromatograms using GC-MS due to insufficient sample material and/or poor solubility. The Py-GC-MS chromatograms clearly showed *Hymenaea*–type labdane diterpenoid composition (not shown). The ChromIdent matches of these samples shows great similarity with *Hymenaea* resin. The inclusion of Burseraceae resin is common in these samples (detection of pentacyclic triterpenoids), but the matrix of the resin figures is clearly composed of *Hymenaea* material. The weak GC-MS signal for most samples might indicate insolubilization due to diagenetic polymerization of the resin. These results show that for archaeological samples Py-GC-MS can be useful to release polymerized resin materials.

In conclusion, all the resin figurines are probably composed of *Hymenaea* resins with various inclusions or absorbed substances such as vegetable fats, Burseraceae resin (probably from *B. tomentosa*) and an unidentified resin (sample RESIN_03). The presence of burseraceous resin in most *Hymenaea*-based figurines would imply deliberate mixing of different botanical sources.

3.2.2. Golden objects

The samples GOLD_01, GOLD_02 and GOLD_03 did not produce meaningful fingerprints using Py-GC-MS, after several attempts varying the amount of introduced sample, which discards a major organic matter content. Sample GOLD_01 consistently produced elemental sulphur suggesting that it contains a S-bearing mineral phase. Using GC-MS, these three samples only produced a series of fatty acids, glycerols and oleamide, which probably indicate degraded lipids. These results show that for tracing the lipid composition in samples with dominant inorganic matrices, GC-MS after isolation by solvent extraction is much more sensitive.

The other samples from this group, i.e. GOLD_04, GOLD_05 and GOLD_06, yielded GC-MS and Py-GC-MS chromatograms that are dominated by a series of n-alkanes and n-alkenes (C_{10}–C_{33}) (Figs. 3–5). Peaks of C_{28}–C_{32} alkanols were also detected by GC-MS and THM-GC-

MS, and to a lower extent by Py-GC-MS. With Py-GC-MS, the alkane/alkanol signal was accompanied with minor peaks of fatty acid methyl esters (C_{28}–C_{32} FAMEs), suggesting the presence of ester bonds. THM-GC-MS (GOLD_04 and GOLD_05 only) also produced large amounts of alkanes, in addition to FAMEs (Fig. 5). Hence, the infillings of these artefacts are composed of wax materials. The presence of free alkanes in combination with FAMEs with abundant C_{20}–C_{24} (in sample GOLD_04, the peak for C_{22} FAME is larger than those of the omnipresent C_{16} and C_{18} FAMEs) and detection of the methylated (THM-GC-MS) and silylated (GC-MS) C_{30} alkanol suggest that the wax is beeswax (Heron et al., 1994; Evershed et al., 1997; Regert et al., 2001; Łucejko et al., 2017), because C_{30} alkanol is indicative of myricyl palmitate (Garnier et al., 2002). However, (epicuticular) plant waxes cannot be discarded as a possible minor source especially of the free alkane fraction (Asperger et al., 1999). The presence of these peaks suggests that the material had not been subjected to significant heating (*cf.* Regert et al., 2001). It is likely that the wax conveyed exceptional plasticity to these samples: contrary to any others, GOLD_04–GOLD_06 were grey-coloured black-mottled moldeable materials.

The presence of amyrins after Py-GC-MS (Table 3), which was also reflected by many ChromIdent markers (pentacyclic triterpenoids of type PT1 and PT2 and unidentified compounds with m/z 157 and 242) (Table 4), and after THM-GC-MS (Fig. 5) of GOLD_04 and GOLD_06 probably reflects the presence of Burseraceae triterpenoids. The proportions of aforementioned pentacyclic terpenoid product types PT1–PT4 strongly suggest *B. tomentosa*-like resin rather than *B. simaruba* or *T. panamensis*. GC-MS confirmed presence of amyrins and lupeol (fingerprint similar to *B. tomentosa*) in GOLD_04 and GOLD_06 (not shown). GOLD_04 showed a larger number of pentacyclic triterpenoid peaks than the other samples, possibly indicative of stronger diagenetic alteration (isomerization). ChromIdent linked GOLD_04 and GOLD_05 to *Hymenaea*, but only in the case of GOLD_05 is this evidence considered strong enough to infer presence of *Hymenaea*-like resin (presence of

Table 4
Results from ChromIdent using the Py-GC-MS data of the archaeological samples and the extant resin pyrolyzates. Bold numbers are considered likely recognition of the corresponding resin's fingerprint by the tool (after checking marker value in the original chromatograms).

Sample	Parameter	Bursera	Tetragastris	Copaifera	Hymenaea
RESIN_01	overall match	2	3	0	**43**
(a)	reverse matches	4	8	0	**53**
	markers	1	0	3	**20**
RESIN_02	union matches	2	3	0	**38**
	reverse matches	4	7	0	**54**
	markers	1	0	3	**26**
RESIN_03	union matches	1	2	1	**56**
	reverse matches	4	7	4	**69**
	markers	1	0	4	**26**
RESIN_04	union matches	1	2	0	**18**
	reverse matches	3	28	18	**47**
	markers	1	0	3	**9**
RESIN_05	union matches	2	1	0	**32**
	reverse matches	2	5	0	**39**
	markers	0	1	4	**19**
RESIN_06	union matches	1	2	0	**27**
	reverse matches	3	6	0	**53**
	markers	1	1	4	**20**
RESIN_07	union matches	1	2	0	**16**
	reverse matches	3	7	0	**44**
	markers	1	1	3	19
GOLD_04	union matches	**1**	0	0	0
	reverse matches	**4**	1	0	6
	markers	**9**	0	0	4
GOLD_05	union matches	**4**	0	0	**3**
	reverse matches	**21**	1	3	12
	markers	**7**	1	0	4
GOLD_06	union matches	**1**	0	0	0
	reverse matches	**3**	0	0	1
	markers	**9**	0	0	2
BODY_03	union matches	0	0	0	3
	reverse matches	0	0	0	4
	markers	1	0	0	2
BODY_04	union matches	**1**	0	0	0
	reverse matches	**1**	0	0	1
	markers	**4**	1	0	3
BODY_05	union matches	1	1	0	**3**
	reverse matches	2	4	0	**6**
	markers	3	0	0	**6**

DLAP using Py-GC-MS; traces of iso-ozic, copalic/kolavenic and eperuic acid confirmed in partial ion chromatograms of GC-MS). GOLD_05 also produced a series of unidentified terpenoids (described earlier for the RESIN_03 figurine) (Fig. 4). Besides wax and burseraceous resin, GOLD_04 and GOLD_06 appear to contain another unidentified resinous material (a series of compounds with m/z 205–290, 207–292, 223–306 and 313–328; THM-GC-MS). These results probably indicate that the golden object infillings not only contained a (bees)waxy basis and burseraceous resin, but also resin of *Hymenaea* and several types of unidentified resins, indicative of extraordinarily complex mixtures.

3.2.3. Tomb sediments and body adhesives

BODY_01 did not produce meaningful indicators of organic substances by Py-GC-MS, which implies that it was probably not a resin fragment (initial label during excavation). As for other samples with no significant Py-GC-MS signal, GC-MS showed the presence of a series of fatty acids and glycerol derivatives of fatty acids indicative of degraded lipids.

BODY_02 showed the aforementioned lipid products and a series of sesquiterpenes by GC-MS (tentative identification of isolongifolol, copaene, calamenene and muurolene, among others), which could point towards the presence of Fabaceae exudate (*Copaifera* or *Hymenaea* resin, which cannot be distinguished easily in this case because the resin signal is weak). Using Py-GC-MS, some aliphatic products (alkanes/alkenes, but with low intensity and narrow chain length range between C_{10} and C_{25}, i.e. not from wax), alkylbenzenes and PAHs including naphthalenes probably indicate presence of soil organic matter (SOM) that is not associated with the body adhesives or human remains. The PAHs may suggest presence of pyrogenic SOM (fire residues) (González-Vila et al., 2001; González-Pérez et al., 2004). We have no explanation for the lack of sesquiterpenoid signal by Py-GC-MS. Perhaps the concentration is too low or interference by inorganic material during pyrolysis mitigated the release of these products (cf. Zegouagh et al., 2004).

The GC-MS signals of sample BODY_03 (unspecified material from bottom of Tomb 4, in contact with corpse) and BODY_04 (resin in contact with same body) were strongly dominated by the pentacyclic triterpenoid products of Burseraceae (α-amyrin, α-amyrone and lupeol), especially *Bursera tomentosa*, accompanied with a minor sesquiterpenoid fraction. The same fingerprints were obtained by Py-GC-MS, but with sesquiterpenoids being much more abundant than amyrins, probably due to poor detection of the latter. Furthermore, sample BODY_03 contained a non-burseraceous resin fraction similar to that of GOLD_04. Sample BODY_05 produced unidentified higher molecular weight resinous compounds (not labdanes) but also monoterpenes such as cymene upon pyrolysis, and using GC-MS the intense amyrin signal is accompanied with some products that have not been identified in other samples (triterpene 24-noroleana-3,12-diene and sesquiterpenes identified tentatively as neoclovenes). Vegetable lipids including oleamide and octadecanamide were relatively abundant in the GC-MS chromatogram of BODY_04. The ChromIdent matches support a presence of Burseraceae resin in sample BODY_04 and perhaps the other two samples, and *Hymenaea*-like resin in BODY_05. The main conclusion that can be drawn from these results is that the bodies from Tomb 4 were treated (e.g. shrouding) with burseraceous resin, perhaps *Hymenaea*-like resin and an additional, unspecified terpenoid constituent in samples BODY_03 and BODY_05.

3.3. Archaeological Hymenaea material: resin or amber

The results showed the presence of *Hymenaea*-derived resin materials. Alteration of this resin can be related to (1) the initial polymerization reactions during drying and hardening of the resin, (2) diagenesis of the hardened resin in the tomb environment, or (3) geological fossilization (amber resinite formation). The distinction between modern *Hymenaea* resin, ancient resin ("copal") and amber is not straightforward (Anderson, 1996; Stankiewicz et al., 1998). In order to make an estimation of the state of the archaeological resin we analyzed a sample of Mexican amber (from extinct *Hymenaeae* spp.) using Py-GC-MS, THM-GC-MS and FTIR.

The Py-GC-MS and THM-GC-MS data of extant *Hymenaea courbaril* resin showed clear signs of early alteration such as the presence of DLAP. These compounds reflect partial but rapid modification or elimination of the exocyclic olefin chain, and can be related to early polymerization reactions (Clifford and Hatcher, 1995) and is probably associated with the reactivity of *enantio* labdanes and in particular (iso-)ozic acid (Mills and White, 2015). The hardening of the resin is thus associated with significant chemical changes that occur virtually instantaneous, i.e. a matter of days/weeks (Solórzano-Kraemer et al., 2018). Hence, we will make no attempt to distinguish fresh resin and copal (for *Hymenaea*, also referred to as *animé*), just between "resin" and "amber".

The additional Py-GC-MS and THM-GC-MS chromatograms recorded

for of extant resin, Mexican amber and sample RESIN_02, show that the labdane acids are clearly depleted in the fossil resin (Fig. 7), which can be explained by defunctionalization reactions (Clifford and Hatcher, 1995). The higher abundance of condensed bicyclic aromatic compounds (mostly trimethyl and dimethyl-methylethyl naphthalenes) indicate extensive condensation of the cyclic moieties as well (McCoy et al., 2017). In fact, the relatively high molecular weight diterpene acid fraction is completely absent in chromatograms of amber.

From the Py-GC-MS and THM-GC-MS datasets, we considered two ways to estimate the degree of diagenetic alteration of *Hymenaea* resins. Firstly, using THM, three of the most abundant labdanoid structures with intact (methylated) carboxylic group are eperuic acid, copalic acid and iso-ozic acid. These compounds are formed upon THM of extant resin and Colombian copal samples, but not from Mexican amber. For THM-GC-MS of the archaeological samples, only results for object RESIN_02 were obtained. A proposed proxy of decarboxylation (% of three labdane acids to sum of labdane products) shows a 4% decarboxylation of the extant resin, 1% for Colombian copal and 100% for Mexican amber. The archaeological sample RESIN_02 has a decarboxylation degree of 20%. This suggests that some defunctionalization occurred during ca. 1000 yrs of storage in the sediment (or manufacturing of the figurine), but that decarboxylation is only in an initial phase in comparison with geological diagenetic alteration, and that the archaeological sample is not comprised of amber.

The second approach is based on the ratio between the biformene-derived hydronaphthalenes C_4-tetrahydro- and C_4-octahydronaphthalene (Clifford and Hatcher, 1995), and can be computed for both Py-GC-MS and THM-GC-MS, as these compounds are released from both reactions. The ratio is partially based on McCoy et al. (2017), who identified C_4-tetrahydronaphthalene as a marker of condensation of *Hymenaea* resin due to its diagenesis to amber, by means of Principal Component Analysis. The large difference in the abundance of this compound between amber and resins was also observed in the present study. A simple proxy on the basis of condensation degree of the resin is obtained from 100% * (C_4-tetrahydronapthalene/(C_4-tetrahydronapthalene + C_4-octahydronapthalene). Using the THM-GC-MS data, the degrees of condensation were 24–53% for extant resin, 18% for Colombian copal, 89–100% for amber samples and 6% for the RESIN_02 fragment. From Py-GC-MS, a similar picture was obtained: 29–63% for extant resin, 40% for Colombian copal, 98% for Mexican amber and 7% for RESIN_02 for this index. This indicates that the degree of condensation for resin (and this archaeological resin) is in the low range whereas that of amber is in the high range. The usefulness of these proxies will be stressed by future investigations.

Another way to evaluate the resins was to calculate linear correlation coefficients between the Py-GC-MS fingerprints of archaeological resins, extant *Hymenaea* resin and amber specimen, using the 55 terpenoid compounds that were semi-quantified. Fig. 8 shows that the resin figurines and bead (RESIN_01–RESIN_07) correlate significantly to the fingerprints of both extant and fossil resin. The large differences between subsamples of RESIN_01 shows that this parameter is not very sensitive to differences in maturity as heterogeneity in terms of maturity is not expected within one fragment (but not impossible; Coty et al., 2014; Martínez-Delclòs et al., 2004). This approach confirmed some
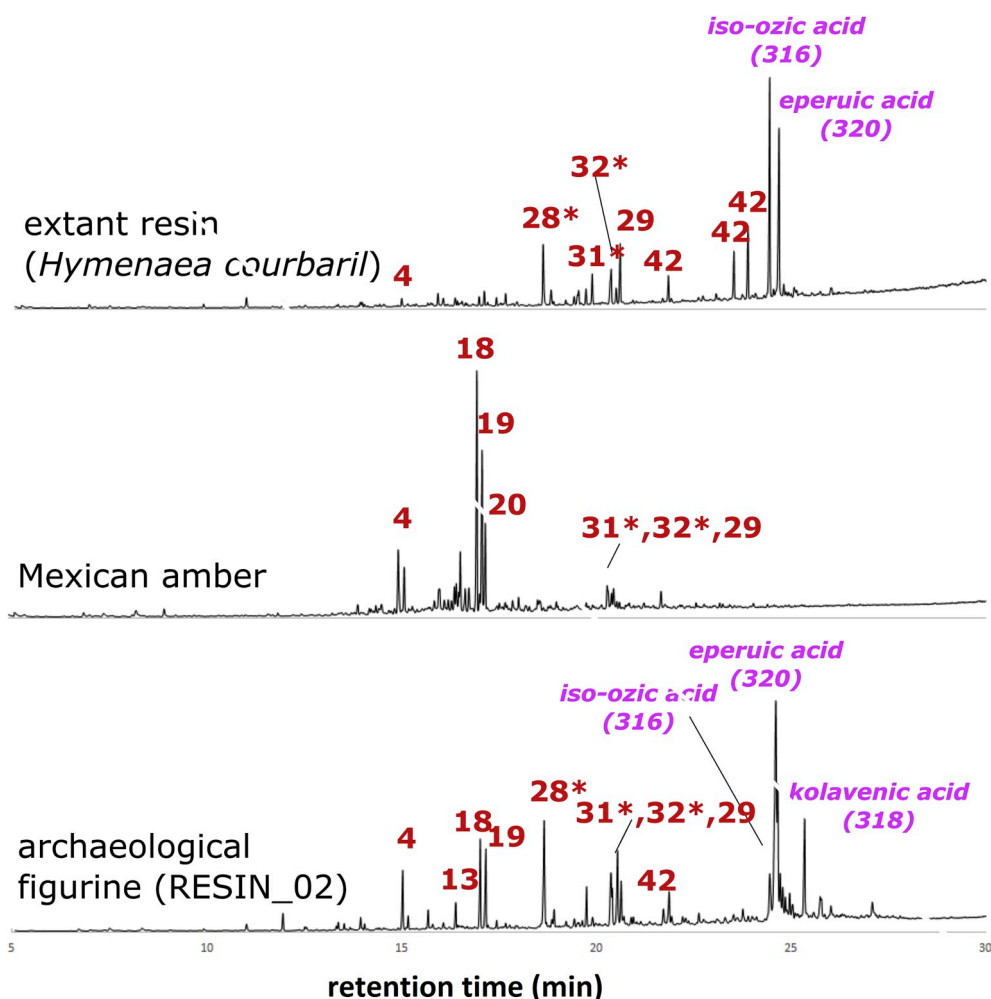
Fig. 7. THM-GC-MS chromatograms of extant resin, Mexican amber and archaeological resin figurine RESIN_02.
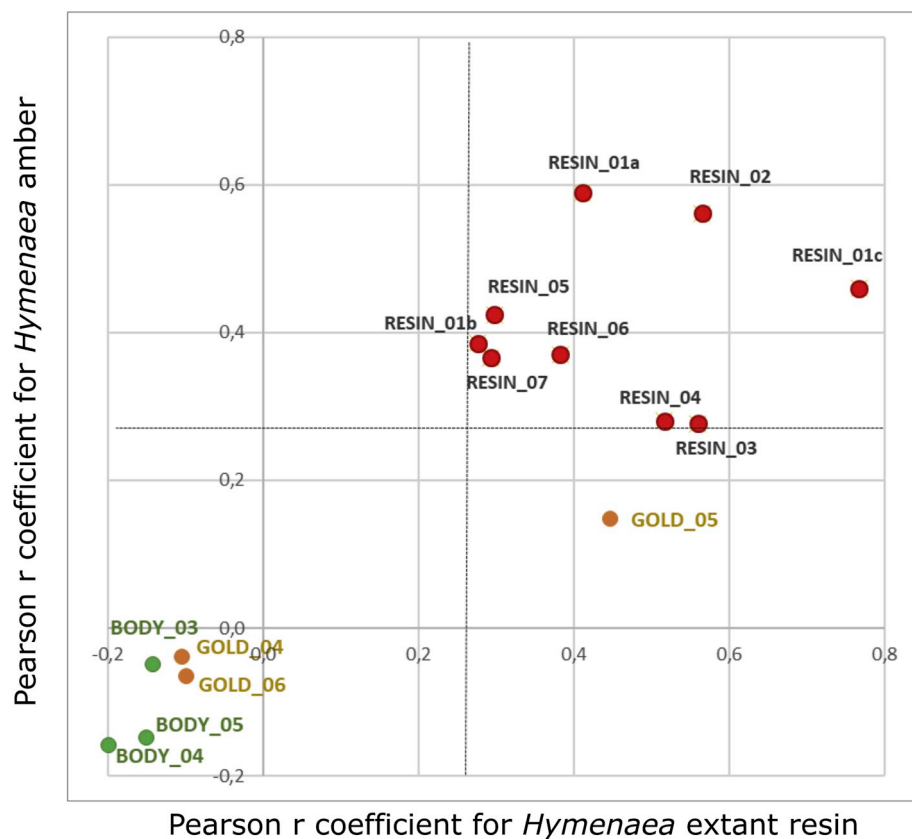
Fig. 8. Representation of correlation analysis for Py-GC-MS fingerprints of archaeological samples (sample codes in Table 1): x-axis is the r coefficient for the pyrolysis fingerprint of the archaeological sample and that of extant resin, whereas the y-axis shows the coefficient for the archaeological sample and Mexican amber sample. R values > 0.27 (or < -0.27) are significant at $P < 0.05$.

resemblance between the resin in GOLD_05 and extant *Hymenaea* resin (Fig. 8).

The study by FTIR aimed to obtain an independent validation of *Hymenaea* resin as the main constituent of the resin figurines (RESIN_02) and to assess the degree of condensation (resin *vs.* amber). Besides the target archaeological sample, RESIN_02, Colombian copal and Mexican amber samples were used as reference (Fig. 9). The main absorption peaks and their proposed assignments are listed in Table 5. Natural resins are similar in band position and intensity of signals pattern in
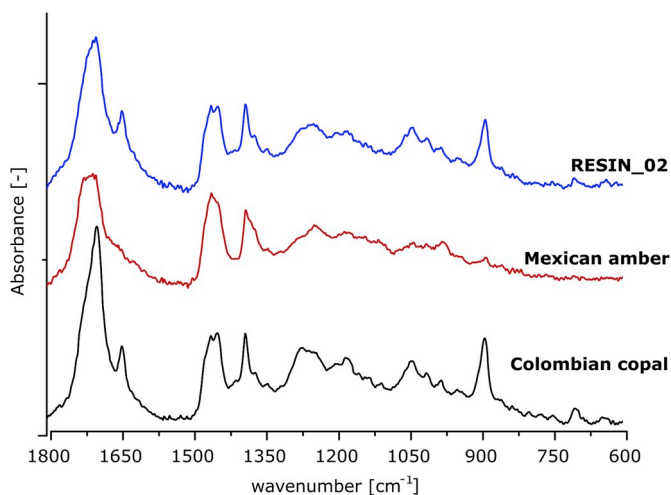
Fig. 9. Partial (1800-600 cm^{-1}) FTIR (ATR) spectra of Colombian copal, Mexican amber and archaeological sample RESIN_02.

region 3500–2850 cm^{-1} including undiagnostic bands of the strongest intensity from symmetric and asymmetric stretching vibrations of methyl (~2970 and ~2860 cm^{-1}) and methylene (~2930 and ~2850 cm^{-1}) residues, the νOH band (~3400 cm^{-1}) and signal(s) at 3070 cm^{-1} corresponding to $\nu = $C–H vibrations (Supplementary Information 3). The fingerprint region (1300–900 cm^{-1}), extended to include the carbonyl stretching vibration band(s) at 1740–1695 cm^{-1} (Wagner-Wysiecka, 2018) shows one of the most characteristic features of spectra of *Hymenaea* resins is the "wave-shaped" region at 1050–920 cm^{-1} (Langenheim and Beck, 1965) of different relative intensities of bands depending on the type of resin (Fig. 9). For *Hymeneae* resins the most characteristic bands in fingerprint region are the νC $= $O signal (often as two bands: ~1700 and 1695 cm^{-1}) and δC-O band (~1260 cm^{-1}), which can be observed in all spectra (Fig. 9). The relatively intensive band of γ vinylidene group deformation vibrations (out of plane) at 888 and δC $= $C band at 1643 cm^{-1} (Kosmowska-Ceranowicz, 2015) point the presence of unsaturated moieties, which indicates the low degree of maturation of the resin. Furthermore, non-fossil *Hymenaea* resins show a clear band at 700 cm^{-1} (unassigned skeletal vibrations), which is absent in amber (Langenheim and Beck, 1965; Swain, 1970). On the basis of these criteria, and comparison with an unpublished collection of reference spectra (Supplementary Information 3), the identity of the Colombian copal sample as *Hymenaea* resin is confirmed. For Mexican amber, the νC $= $O band is localized at 1715 cm^{-1} and the δC-O vibration signal is observed at 1242 cm^{-1}. The shift of bands assigned to carbon-oxygen bonds towards higher wavenumber values, and the absence of signals at 888 and 700 cm^{-1} indicate significant maturity and saturation, which allows to classify it as fossil resin, and comparison with reference collection spectra to Mexican amber in particular (Supplementary Information 3). Spectral properties of the archaeological sample that was available, i.e. RESIN_02, are

Table 5
The main absorption peaks in the spectra and proposed assignments.

Band assignment	Colombian copal	Mexican amber	RESIN_02
Unsaturated moieties vibrations			
$\nu = $C–H	3080, 3073, w	nb	3080,3073, w
ν –C$\equiv$C- alkenyl	1643,m	~1664, sh	1643, m
γRHC = CH$_2$ vinyl	978, w	989, w, sh	988-976, w
γR2C$\equiv$CH$_2$ vinylidene	887, w	888, very w	887, m
Saturated C–H moieties vibrations			
νC-H in: –CH$_2$ - and CH$_3$ groups	2930, s	2924, s	2930, s
	2866, m	2880, m	2866, m
	2850, m	2865, m	2844, s
δC-H in –CH$_3$ and –CH$_2$-	1458, 1448, m	1456, m	1457, 1444, m
δC-H in –CH$_3$	1390, m	1385, m	1389, m
Unassigned skeletal vibrations	700, w	nb	701, w
Oxygen bearing moieties			
νOH alcohols and carboxylic acids - (hydrogen bonded)	~3414, m, b	~3330, very w, b	~3414, m, b
γO-H carboxylic acids	945, 936, 930, m-w, b	946, 939, 935 w, b	946, 938, m-w, b
νC = O carboxylic acids (hydrogen bonded)	1696, m	1710, m-s	1709 w, sh 1697, m
νC-O carboxylic acids	1268, 1255, 1244, 1238, m-w	1242, m-w	1267, 1254, 1243, 1237, m-w
νC-O carboxylic acids and 2° alcohols[a]	1194, 1177, 1150, 1102, m-w	1191, 1179, 1171, 1102, m-w	1194, 1174, 1166, 1150, 1102, m-w
νC-O 1° and 3° alcohols[a]	1042, 1038, 1008, m-w	1041, 1035, 1009, m-w	1053, 1037, 1008, m-w

Relative intensity: s - strong, m - medium, w - weak, b - broad, sh - shoulder, nb - no band. Vibrations: ν - stretching, δ - deformational in plane, γ - deformational off the plane, as-asymmetric, sym-symmetric.

[a] Region of overlapping of different functional groups e.g. γC-C skeletal vibrations.

similar to those of the reference materials (Fig. 9, Table 5). A general assessment of the degree of maturation (notwithstanding the natural diversity of material composition within amber deposition) is provided by the ratio of the relative intensity (normalized spectra) of signals attributed to unsaturated and saturated moieties, i.e. the ratios of signals $888/1388 \, \text{cm}^{-1}$ and $888/1458 \, \text{cm}^{-1}$ (Supplementary Information 3) increase in the order Mexican amber > RESIN_02 > Colombian copal. From the data it is concluded that RESIN_02, can be classified as ancient, non-fossil, resin.

In conclusion, there are several indications of a significant degree of polymerization and defunctionalization of the *Hymenaea* resin's labdane fraction of the archaeological samples, but combined evidence clearly shows that the archaeological resins are non-fossil.

3.4. Resin and cerumen in pre-Columbian funerary contexts of Panama

It was shown that the main constituent of the figurines and beads is the resin of *Hymenaea*. *Hymenaea courbaril* is a tall tree that grows in the drier regions of the isthmus, frequently in riparian forests (Condit et al., 2011). Its seeds are surrounded by edible pulp that was consumed during the Middle to Late Ceramic (400 BC-AD 1500) in Panama (Dickau, 2010). Among American indigenous groups the resin or copal produced by this tree was used as incense, insect repellent, and/or in folk medicine (Gupta et al., 1979; Case et al., 2003; Pennacchio et al., 2010). The members of the *Hymenaea* genus, especially *H. courbaril* (Caribbean Island, South and Central America) and *H. verrucosa* (Madagascar and East Africa) have exceptional properties in terms of resin productivity, polymerization rate and hardness, and many uses of its copals and ambers have been reported in archaeological literature (e.g. Anderson et al., 1992; Langenheim, 1995; McCoy et al., 2017; Crowther et al., 2015). The use of *Hymenaea* as raw material for crafting

resin beads, pendants and figurines dated since cal. AD 700–1400 has been proposed for objects recovered from different burial grounds of Costa Rica (Stone, 1963; Langenheim and Balser, 1975) and for beads recovered from Lake Guatavita in Colombia (Anderson and Bray, 2006). Furthermore, *Hymenaea* bark, fruits, resin, leaves, seeds, and stems have several ethnopharmacological uses (Boniface et al., 2017). An infusion of the bark is taken by Panamanians to relieve multiple diseases such as rheumatic pain, diabetes, gastrosis, oral ulcers, and hypoglycemia (Duke et al., 2009), the fruits are consumed to treat mouth ulcers and the leaves for diabetes (Gupta et al., 1979).

It cannot be discarded that the *Hymenaea* resin fingerprints may be shared by other species that are not part of the reference database, in the same way that amyrins are only "markers" of Burseraceae if other producers of such compounds, mostly Fabaceae such as *Acacia* spp., are not considered. Here we rely on the ethnobotanical record used to select the most likely sources of resins and other materials (Langenheim, 2003; Case et al., 2003; Pennacchio et al., 2010), as well as historical sources such as the reports of Columbus (1494) to the Catholic Monarchs during his second voyage to the Western Indias that has been interpreted (Langenheim, 2003) as a reference to the resin produced by *Hymenaea*. Nevertheless, future extension of the reference collection might allow identification of hitherto unidentified resins or suggest better candidates for tentatively identified sources of the present study, e.g. *Humiriastrum diguense* that has been described as embalming resin in the Caribbean coast of Panama (Griggs, 2005; Dickau, 2010). The presence of degraded lipidic structures in some of the samples may have different explanations, including the manipulation of the resin during molding (resin was heated in order to create figurines, and fingerprints have been identified; Victoria-Lona, 2012), or during archaeological excavation.

Of the golden object infillings, three samples produced unequivocal fingerprints of wax material, in all likelihood that of beeswax. Currently, the most comprehensive explanation of the coexistence of wax and terpenoid materials in these items is the use of cerumen (a mixture of wax, resins and gums), which is naturally charged with plant resin (collected as an antimicrobial sealant; Leonhardt, 2017). Wax and cerumen are produced by stingless bees (Apidae: Meliponini) which are native to the tropical region (Nogueira-Neto, 1997; Jones, 2013; Quezada-Euán et al., 2018) and abundant in Panama (Michener, 1954). Meliponini use cerumen for building their nests, mixing secreted wax with natural terpenoids present in the plant products collected from trees and shrubs (Leonhardt et al., 2009). These resins and other additives darken the wax, giving rise to a light yellowish to almost black colour (Nogueira-Neto, 1997), receiving the common name "black beeswax" (Stearman, 1989). The culture of social bees and their management in hives (meliponicultura) is well-documented for Mayan communities that had a deic entity of the bees (Ah-Muzen-Cab) (Crane, 2001; Hrncir et al., 2016). Beekeeping has been also described in the Azuero peninsula in Western Panama (Kent, 1984). The symbolic and economic relevance (including complex exchange networks) of stingless bees has been attested for indigenous communities around Colombia, such as the Andocke (Jara, 1996), the Muisca and the U'wa (Falchetti, 1997, 2003; Falchetti and Nates-Parra, 2002). Beeswax material produced by stingless bees was commonly used for crafting by American indigenous cultures: 1) for producing models of golden jewels by the practice of lost-wax casting (Bray, 1978; Jones, 2013) mostly outside the Mayan area (Quezada-Euán et al., 2018); 2) as an adhesive for feathers and beads arts (Stearman et al., 2008; Ayala et al., 2013) and 3) for waxing threads to bind arrows (Ruddle, 1973). For the golden objects from El Caño, the physical properties of the infillings (especially its moldeability) and the very intense signal of wax suggest that the wax is not merely an adhesive or a residue of wax-based threads, but a key ingredient of the infilling itself, and therefore it should be considered as a raw material or a result of lost-wax casting.

The results of the present study clearly stress the complexity of the bee-oriented metallurgical technology of these communities which involved the use of cerumen associated with golden objects, which is

different for GOLD_05 (unidentified resin, *Hymenaea*) and GOLD_04/ GOLD_06 (Burseraceae and another unidentified resin). Note that the unidentified resin in GOLD_05 has the same molecular structure as that of sample RESIN_03, but its source has not been recognized yet. The presence of burseraceous resin in Meloponini cerumen was reported by Massaro et al. (2011), but resins from *Hymenaea courbaril* predominate (Nogueira-Neto, 1997). The relevance of wax material in goldwork has been recently highlighted through a combination of technical analyses of Colombian metalwork and ethnographic data (Martinón-Torres and Uribe-Villegas, 2015). This proposal is partially based on the complex symbolism of gold, as well as the crucial role of stingless bees and bees' products in the cosmology of Colombian indigenous communities (Falchetti, 1997, 2001; 2003; Falchetti and Nates-Parra, 2002). Secondary uses of cerumen involved traditional medicine practiced by shamans and midwives, e.g. the Kayapó in Brasil burn the cerumen to produce smoke to attract storm clouds and rain, as well as to repel evil spirits (Quezada-Euán et al., 2018).

Regarding the use of resins for manipulating the dead bodies, the most relevant results are those provided by sample BODY_02 recovered from the main individual of Tomb 2. This high-ranking individual was deposited in ventral decubitus and was previously desiccated and shrouded (Mayo Torné et al., 2016). The results indicate the presence of Fabaceae-Caesalpinoideae exudates in direct contact with the body that could corroborate the previous hypothesis, based also in the ethnohistorical sources such as the descriptions of this kind of mortuary practice by Fernández de Oviedo (1853: 155). The presence of other resins including burseraceous ones in samples recovered from Tomb 4 points towards a widespread use of resins during the funerary ritual. The Burseraceae family includes over 20 genera of trees and scrubs from tropical and subtropical regions from Asia, Africa and America (Daly et al., 2010). *Bursera* species are highly resinous, and their resins have been widely used as a raw material for crafting and as incense for burning, amongst other uses including those of traditional medicine (Lucero-Gómez et al., 2014). In Panama, *Bursera tomentosa* is found only in the driest areas of the country (Condit et al., 2011). The samples of El Caño allowed, for the first time, the identification of Burseraceae resins in the funerary treatment of the bodies, probably as embalming agents. Hitherto only conifer resin had been identified in textile bands wrapping Inca mummies from Peru (Degano and Colombini, 2009).

This multidisciplinary research highlights the complex management of plant resources developed by indigenous communities that inhabited the Pacific slope of Panama in the period comprised between cal. AD 700–1020, which is in agreement with archaeobotanical analyses of charcoal remains from funerary contexts (Martín-Seijo et al., 2016, 2018). The central role of trees in the cosmologies of current Panamanian indigenous communities (Velásquez-Runk, 2009) as well as the material and symbolic entanglements with plant-based objects (Martínez-Mauri, 2020) has been also described in anthropological research. The molecular evidence indicates multiple uses of plant exudates, in the funerary rituals associated to high-ranking individuals, complementing and perhaps going beyond information provided by ethnohistorical and ethnographic sources. The use and manipulation of the examined resins from El Caño probably involved a complex forest and tree management aimed to the procurement (and perhaps to the exchange or trade) of these plant exudates burned in incense vessels, used for embalming the bodies and for crafting resin objects and infillings for gold-works. Resins were obtained from *Hymenaea* and Burseraceae, probably *B. tomentosa*, amongst other unidentified taxa, both for crafting resin figurines with or without golden linings, and mixed with wax as an infilling of golden beads. The quality of the resin-based items and the simultaneous use of a variety of materials for their creation, should be considered as evidence of the existence of craft specialists. For the Pre-Columbian communities that created these materials, the cultural relevance and symbolic importance of wax, and perhaps resin, may be as important as the metals themselves (Hastorf, 1999; Martinón-Torres and Uribe-Villegas, 2015).

4. Conclusions

A detailed molecular account of the resins from several ethnobotanically important species linked their composition to the resin materials from the tombs in the El Caño burial site. The resin figurines are composed of *Hymenaea*-like resin, possibly of *Hymenaea courbaril*. Combining GC-MS, Py-GC-MS, ChromIdent, THM-GC-MS and FTIR, the molecular state of *Hymenaea*'s labdane diterpenoids was elucidated, showing significant alteration due to initial polymerization and long-term storage in the tombs. Clearly, the resin figurines were not shaped from amber. Furthermore, they contain traces of resin that is similar to that of the Burseraceae studied, *Bursera tomentosa* in particular. The fillings of the golden objects were mainly wax, probably cerumen with the presence of *Hymenaea*-like, Burseraceae-like and several types of unidentified resins, indicative of a complex composition. The use of resins in the treatment of the dead bodies was shown by the presence of various terpenoid materials. Resins probably played a central role in the burial traditions, both for *post-mortem* treatments applied to the dead bodies and for burning during the burial itself. But perhaps the most significant archaeological implication is the evidence of complex man-agement of forest resources developed by these communities, in the period comprised between cal. AD 700–1020. This includes the man-agement of trees to produce plant exudates to be used as raw materials for crafting different objects –pendants, beads and figurines– as well as in funerary treatments that involved the use of resins in direct contact with the deceased. The data obtained also point to the use of stingless bee products such as cerumen in relation to goldsmithing.

References

Anderson, K.B., 1995. The Nature and Fate of Natural Resins in the Geosphere, Part IV: New Evidence Concerning the Structure, Composition, and Maturation of Class I (Polylabdanoid) Resinites. American Chemical Society, pp. 105–129.

Anderson, K.B., 1996. The nature and fate of natural resins in the geosphere – VII. A radiocarbon (^{14}C) age scale for description of immature natural resins: an invitation to scientific debate. Org. Geochem. 25, 251–253.

Anderson, K.B., Bray, W., 2006. The amber of El Dorado: class IB archaeological ambers associated with Laguna Guatavita. Archaeometry 48 (4), 633–640.

Anderson, K.B., Winans, R.E., 1991. Nature and fate of natural resins in the geosphere. I. Evaluation of pyrolysis-gas chromatography mass spectrometry for the analysis of natural resins and resinites. Anal. Chem. 63, 2901–2908.

Anderson, K.B., Winans, R., Botto, R., 1992. The nature and fate of natural resins in the geosphere—II. Identification, classification and nomenclature of resinites. Org. Geochem. 18, 829–841.

Asperger, A., Engewald, W., Fabian, G., 1999. Advances in the analysis of natural waxes provided by thermally assisted hydrolysis and methylation (THM) in combination with GC/MS. J. Anal. Appl. Pyrol. 52, 51–63.

Ayala, R., Gonzalez, V.H., Engel, M.S., 2013. Mexican stingless bees (Hymenoptera: Apidae): diversity, distribution, and indigenous knowledge. In: Vit, P., Pedro, S., Roubik, D. (Eds.), Pot-Honey. Springer, New York, pp. 135–152.

Boniface, P.K., Ferreira, S.B., Kaiser, C.R., 2017. Current state of knowledge on the traditional uses, phytochemistry, and pharmacology of the genus Hymenaea. J. Ethnopharmacol. 206, 193–223.

Bray, W., 1978. Gold-working in ancient America. Gold Bull. 11 (4), 136–143.

Brown, A.E., 2002. *Hymenaea mexicana* sp. nov. (Leguminosae: Caesalpinioideae) from Mexican amber indicates Old World connections. Bot. J. Linn. Soc. 139, 125–132.

Calvillo-Canadell, L., Cevallos-Ferriz, S.R., Rico-Arce, L., 2010. Miocene *Hymenaea* flowers preserved in amber from Simojovel de Allende, Chiapas, Mexico. Rev. Palaeobot. Palynol. 160, 126–134.

Case, R.J., Tucker, A.O., Maciarello, M.J., Wheeler, K.A., 2003. Chemistry and ethnobotany of commercial incense copals, copal Blanco, copal oro, and copal Negro, of North America. Econ. Bot. 57, 189–202.

Challinor, J.M., 2001. Review: the development and applications of thermally assisted hydrolysis and methylation reactions. J. Anal. Appl. Pyrolysis 61, 3–34.

Chiavari, G., Prati, S., 2003. Analytical pyrolysis as diagnostic tool in the investigation of works of art. Chromatographia 58 (9/10), 543–554.

Clifford, D.J., Hatcher, P.G., 1995. Structural transformations of polylabdanoid resinites during maturation. Org. Geochem. 23, 407–418.

Clifford, D.J., Hatcher, P.G., Botto, R.E., Muntean, J.V., Michels, B., Anderson, K.B., 1997. The nature and fate of natural resins in the geosphere—VIII. NMR and Py–GC–MS characterization of soluble labdanoid polymers, isolated from Holocene class I resins. Org. Geochem. 27, 449–464.

Colombini, M.P., Modugno, F., 2009. Organic Mass Spectrometry in Art and Archaeology. John Wiley & Sons, Ltd, Chichester.

Colombini, M.P., Ribecchini, E., Rocchi, M., Selleri, P., 2013. Analytical pyrolysis with in-situ silylation, Py(HMDS)-GC/MS, for the chemical characterization of archaeological and historical amber objects. Herit. Sci. 1, 6. http://www.heritagesciencejournal.com/content/1/1/6.

Condit, R., Pérez, R., Daguerre, N., 2011. Trees of Panama and Costa Rica. Princeton Field Guides, New Jersey.

Cooke, R.G., 1972. The Archaeology of the Western Coclé Province of Panama. PhD Dissertation. Institute of Archaeology and University of London, London.

Cooke, R.G., 1976. Rescate arqueológico en El Caño (NA-20), Coclé. Actas del IV Simposium Nacional de Arqueología, Antropología y Etnohistoria de Panamá. Panamá, Instituto Nacional de Cultura de Panamá, pp. 447–482.

Cooke, R.G., 2004. Rich, poor, shaman, child: animals, rank, and status in the 'Gran Coclé'culture area of pre-Columbian Panama. Behav. Behind Bones Zooarchaeol. Ritual, Relig. Status Identity 271–284.

Cooke, R.G., Isaza, I., Griggs, J.C., Desjardins, B., Sánchez, L.A., 2003. Who crafted, exchanged, and displayed gold in pre-Columbian Panama? In: Quilter, J., Hoopes, J. W. (Eds.), Gold and Power in Ancient Costa Rica, Panama and Colombia. Washington, D.C., Dumbarton Oaks, pp. 91–158.

Coty, D., Aria, C., Garrouste, R., Wils, P., Legendre, F., Nel, A., 2014. The first ant-termite syninclusion in amber with CT-scan analysis of taphonomy. PLoS One 9, e104410.

Crane, E., 2001. Amerindian uses of honey, wax and brood from nests of stingless bees. Acta Am. 9, 5–15.

Crowther, A., Veall, M.-A., Boivin, N., Horton, M., Kotarba-Morley, A., Fuller, D.Q., Fenn, T., Haji, O., Matheson, C.D., 2015. Use of Zanzibar copal (*Hymenaea verrucosa* Gaertn.) as incense at Unguja Ukuu, Tanzania in the 7e8th century CE: chemical insights into trade and Indian Ocean interactions. J. Archaeol. Sci. 53, 374–390.

Daly, D.C., Harley, M.M., Martínez-Habibe, M.C., Weeks, A., 2010. Burseraceae. In: Flowering Plants. Eudicots. Springer, Berlin, Heidelberg, pp. 76–104.

De la Cruz-Cañizares, J., Doménech-Carbó, M.T., Gimeno-Adelantado, J.V., Mateo-Castro, R., Bosch-Reig, F., 2005. Study of Burseraceae resins used in binding media and varnishes from artworks by gas chromatography–mass spectrometry and pyrolysis-gas chromatography–mass spectrometry. J. Chromatogr. A 1093, 177–194.

Degano, I., Colombini, M.P., 2009. Multi-analytical techniques for the study of pre-Columbian mummies and related funerary materials. J. Archaeol. Sci. 36, 1783–1790.

Dickau, R., 2010. Microbotanical and macrobotanical evidence of plant use and the transition to agriculture in Panama. In: Integrating Zooarchaeology and Paleoethnobotany. Springer, New York, pp. 99–134.

Doménech-Carbó, M.T., de La Cruz-Cañizares, J., Osete-Cortina, L., Doménech-Carbó, A., David, H., 2009. Ageing behaviour and analytical characterization of the Jatobá resin collected from *Hymenaea stigonocarpa Mart.* Int. J. Mass Spectrom. 284, 81–92.

Doyle, G.A., 1960. Metal and pottery associations. Panama Archaeol. 3, 48–51.

Duke, J.A., Bogenschutz-Godwin, Ottesen, A.R., 2009. Duke's Handbook of Medicinal Plants of Latin America.

Evershed, R.P., 1993. Biomolecular archaeology and lipids. World Archaeol. 25, 74–93.

Evershed, R.P., 2008. Organic residue analysis in archaeology: the archaeological biomarker revolution. Archaeometry 50 (6), 895–924.

Evershed, R.P., Vaughan, S.J., Dudd, S.N., Soles, J.S., 1997. Fuel for thought? Beeswax in lamps and conical cups from late minoan Crete. Antiquity 71, 979–985.

Falchetti, A.M., 1997. La ofrenda y la semilla: notas sobre el simbolismo del oro entre los Uwa, vol. 43. Boletín Museo del Oro, pp. 3–37.

Falchetti, A.M., 2001. The transformation of the seed: ritual offerings and trade among the Uwa of Colombia. J. Lat.Am. Lore 21 (1), 109–142.

Falchetti, A.M., 2003. The seed of life: the symbolic power of gold-copper alloys and metallurgical transformations. In: Quilter, J., Hoopes, J.W. (Eds.), Gold and Power in Ancient Costa Rica, Panama, and Colombia. Dumbarton Oaks Research Library and Collection, Washington, pp. 345–381.

Falchetti, A.M., Nates-Parra, G., 2002. Las hijas del sol: las abejas sin aguijón en el mundo de los U'wa, Sierra Nevada del Cocuy, Colombia. In: Bogotá, A. Ulloa (Ed.), Rostros culturales de la fauna: las relaciones entre los humanos y los animales en el contexto colombiano. Instituto Colombiano de Antropología e Historia, pp. 175–214.

Fernández de Oviedo, G., 1853. Historia general y natural de las Indias, Islas y Tierra-Firme del Mar Océano. Imprenta de la Real Academia de la Historia.

Garnier, N., Cren-Olivé, C., Rolando, C., Regert, M., 2002. Characterization of archaeological beeswax by electron ionization and electrospray ionization mass spectrometry. Anal. Chem. 74, 4868–4877.

Ghisalberti, E.L., Godfrey, I.M., 1998. Application of nuclear magnetic resonance spectroscopy to the analysis of organic archaeological materials. Stud. Conserv. 43, 215–230.

Gigliarelli, G., Becerra, J.X., Curini, M., Marcotullio, M.C., 2015. Chemical composition and biological activities of fragrant Mexican copal (*Bursera* spp.). Molecules 20, 22383–22394. https://doi.org/10.3390/molecules201219849.

González-Pérez, J.A., González-Vila, F.J., Almendros, G., Knicker, H., 2004. The effect of fire on soil organic matter—a review. Environ. Int. 30, 855–870.

González-Vila, F.J., Tinoco, P., Almendros, G., Martín, F., 2001. Pyrolysis-GC-MS analysis of the formation and degradation stages of charred residues from lignocellulosic biomass. J. Agric. Food Chem. 49, 1128–1131.

Griggs, J.C., 2005. The Archaeology of Central Caribbean Panama. Unpublished PhD Dissertation. University of Texas, Austin.

Gupta, M.P., Arias, T.D., Correa, M., Lamba, S.S., 1979. Ethnopharmacognostic observations on Panamanian medicinal plants. part I. Q. J. Of Crude Drug Res. 17, 115–130.

Hastorf, C.A., 1999. Recent research in paleoethnobotany. J. Archaeol. Res. 7 (1), 55–103.

Hearne, P., Sharer, R.J., 1992. River of Gold-Precolumbian Treasures from Sitio Conte. University of Pennsylvania Museum of Archaeology, Philadelphia.

Hernández Vázquez, L., Palazon, J., Navarro-Ocaña, A., 2012. The Pentacyclic Triterpenes α,β-Amyrins: a Review of Sources and Biological Activities. Phytochemicals - a global Perspective of their Role in nutrition and health. Venketeshwer Rao. IntechOpen. https://doi.org/10.5772/27253.

Heron, C., Nemcek, N., Bonfield, K.M., Dixon, D., Ottaway, B.S., 1994. The chemistry of neolithic beeswax. Naturwissenschaften 81, 266–269.

Hervás Herrera, M.A., 2018. Las estructuras funerarias de El Caño (Coclé, Panamá) entre los siglos VIII y XI. Proceso constructivo y transformaciones postdeposicionales. In: Alcántara, M., García Montero, M., Sánchez López, F. (Eds.), Memoria del 56.° Congreso Internacional de Americanistas. https://doi.org/10.14201/0AQ0251.

Hrncir, M., Jarau, S., Barth, F.G., 2016. Stingless bees (Meliponini): senses and behavior. J. Comp. Physiol. A 202, 597–601.

Jacob, J., Disnar, J.-R., Boussafir, M., Spadano Albuquerque, A.L., Sifeddine, A., Turcq, B., 2005. Pentacyclic triterpene methyl ethers in recent lacustrine sediments (Lagoa do Caçó, Brazil). Org. Geochem. 36, 449–461. https://doi.org/10.1016/j.orggeochem.2004.09.005.

Jara, F., 1996. La miel y el aguijón. Taxonomía zoológica y etnobiología como elementos en la definición de las nociones de género entre los Andoke (Amazonia Colombiana). J. Soc. des Américanistes 82, 209–258. https://doi.org/10.3406/jsa.1996.1637.

Jones, R., 2013. Stingless Bees: a historical perspective. In: Vit, P., Pedro, S., Roubik, D. (Eds.), Pot-Honey. Springer, New York, pp. 219–227.

Kaal, J., Oliveira, C., Martín-Seijo, M., Mayo, J., Mayo, C., 2018. Objetos de resina en los ajuares de El Caño (Panamá): diseño de un protocolo de análisis y primeros resultados. Actas del 56° Congreso Internacional de Americanistas, Salamanca.

Kent, R.B., 1984. Mesoamerican stingless beekeeping. J. Cult. Geogr. 4, 14–28.

Kiemle, D.J., Silverstein, R.M., Webster, F.X., 2019. Spektroskopowe Metody Identyfikacji Związków Organicznych. PWN Warsaw, p. 2019 (in Polish).

Kosmowska-Ceranowicz, B., 2015. Infrared spectra Atlas of fossil resins, subfossils resins and selected imitations of amber. In: Vávra, N. (Ed.), Mineral Names Used for Fossil Resins and Similar Materials, first ed. Polish Academy of Sciences Museum of the Earth in Warsaw, Warsaw, pp. 140–166.

Lambert, J.B., Tsai, C.H., Shah, M.C., Hurtley, A.E., Santiago-Blay, J.A., 2012. Distinguishing amber and copal classes by proton magnetic resonance spectroscopy. Archaeometry 54, 332–348.

Lambert, J.B., Santiago-Blay, J.A., Ramos, R.R., Wu, Y., Levy, A.J., 2014. Nuclear magnetic resonance (NMR) examination of fossilized semi-fossilized and modern resins from the Caribbean Basin and surrounding regions. Life: Excit. Biol. 2, 180–209.

Langenheim, J.H., 1995. Biology of amber-producing trees: focus on case studies of *Hymenaea* and *Agathis*. In: Anderson, K.B., Crelling, J.C. (Eds.), Amber, Resinite, and Fossil Resins. American Chemical Society, Washington, D.C., pp. 1–31.

Langenheim, J.H., 2003. Plant Resins: Chemistry, Evolution, Ecology, and Ethnobotany. Timber Press.

Langenheim, J.H., Balser, C.A., 1975. Botanical origin of resin objects from aboriginal Costa Rica. Vinculos. Rev. Antropol. Museo Nacl. Costa Rica 1 (2), 72–82.

Langenheim, J.H., Beck, C.W., 1965. Infrared spectra as a means of determining botanical sources of amber. Science 149, 52–55.

Larkin, P., 2011. Infrared and Raman Spectroscopy. Principles and Spectral Interpretation. Elsevier, Amsterdam, p. 230.

Leonhardt, S.D., 2017. Chemical ecology of stingless bees. J. Chem. Ecol. 43 (4), 385–402.

Leonhardt, S.D., Blüthgen, N., Schmitt, T., 2009. Smelling like resin: terpenoids account for species-specific cuticular profiles in Southeast-Asian stingless bees. Insectes Sociaux 56 (2), 157–170.

Linares, O.F., 1977. Ecology and the arts in ancient Panama: on the development of social rank and symbolism in the central provinces. Stud. Pre-Columb. Art Archaeol. 17, 1–86.

Lothrop, S.K., 1934. Archaeological investigation in the province of Coclé. Panamá. Am. J. Archaeol. 38, 207–211.

Lothrop, S.K., 1937. Coclé: an Archaeological Study of Central Panama. Historical Background Excavations at the Sitio Conte: Artifacts and Ornaments. Part 1. Memoirs of the Peabody Museum of Archaeology and Ethnology 7, Cambridge.

Lucero-Gómez, P., Mathe, C., Vieillescazes, C., Bucio, L., Belio, I., Vega, R., 2014. Analysis of Mexican reference standards for *Bursera* spp. resins by gas chromatography-mass spectrometry and application to archaeological objects. J. Archaeol. Sci. 41, 679–690.

Martín-Seijo, M., Piqué i Huerta, R., Mayo Torné, J., Mayo Torné, C., Abad Vidal, E., 2016. Madera carbonizada en contextos funerarios de la jefatura de Río Grande, Panamá: antracología en el sitio de El Caño. Chungará (Arica) 48 (2), 277–294.

Martín-Seijo, M., Mayo Torné, J., Mayo Torné, C., 2018. Madera para acompañar la muerte: antracología en los contextos funerarios de El Caño (Coclé, Panamá). In: Alcántara, M., García Montero, M., Sánchez López, F. (Eds.), Memoria del 56.° Congreso Internacional de Americanistas, ISBN 978-84-9012-913-5. https://doi.org/10.14201/0AQ0251.

Martínez-Mauri, M., 2020. Things, life, and humans in gunayala (Panama): talking about molas and nuchus inside and outside guna society. In: Halbmayer, E. (Ed.), Amerindian Socio-Cosmologies between the Andes, Amazonia and Mesoamerica toward an Anthropological Understanding of the Isthmo-Colombian Area. Routledge, London.

Martinón-Torres, M., Uribe-Villegas, M.A., 2015. Technology and culture in the invention of lost-wax casting in South America: an archaeometric and ethnoarchaeological perspective. Camb. Archaeol. J. 25 (1), 377–390. https://doi.org/10.1017/S0959774314001164.

Martínez-Delclòs, X., Briggs, D.E., Peñalver, E., 2004. Taphonomy of insects in carbonates and amber. Palaeogeogr. Palaeol. 203, 19–64.

Mason, J., 1940. Ivory and resin figures from Coclé. Univ. Mus. Bull. 8 (4), 13–21.

Massaro, F.C., Brooks, P.R., Wallace, H.M., Russell, F.D., 2011. Cerumen of Australian singles bees (*Tetragonula carbonaria*): gas chromatography-mass spectrometry fingerprints and potential anti-inflammatory properties. Naturwissenschaften 98, 329–337.

Mayo, J., Carles, J.A., 2015. Guerreros de Oro: Los Señores de Coclé. Caribe, Panamá.

Mayo, J., Mayo, C., 2013. El descubrimiento de un cementerio de élite en El Caño: indicios de un patrón funerario en el valle del Río Grande, Coclé, Panamá. Arqueol. Iberoam. 20, 3–27.

Mayo, J., Mayo, C., 2013. La escultura precolombina del Área Intermedia. Aproximación al estudio estilístico, iconográfico y espacial del grupo escultórico de El Caño. In: Melgar, E., Solís, R., González, E. (Eds.), Producción de bienes de prestigio ornamentales y votivos de la América Antigua. Syllaba Press, Florida, pp. 12–21.

Mayo, J., Mojica, A., Ruiz, A., Moreno, E., Mayo, C., De Gracia, G.I., 2007. Estructuras arquitectónicas incipientes y áreas de explotación minera prehispánica de las cuencas de los ríos Grande y Coclé del Sur, Panamá. Rev. Española Antropol. Am. 3, 93–110.

Mayo, J., Mayo, C., Guinea, M., 2019. Funerary rituals among the elite of the Río Grande chiefdom, Panama: preparations for the final journey of a powerful Coclé warrior. in press. In: McEwan, Colin, Cockrell, Bryan, Hoopes, John W. (Eds.), Central American and Colombian Art at Dumbarton Oaks (Pre-columbian Art at Dumbarton Oaks, No. 5). Dumbarton Oaks, Washington, D.C.

Mayo Torné, J., Mayo Torné, C., Guinea Bueno, M., Hervás Herrera, M.Á., Herrerín López, J., 2016. La tumba T7 de la necrópolis de El Caño, tradición arqueológica Gran Coclé, istmo de Panamá. Arqueol. Iberoam. 30, 30–43.

McCoy, V.E., Boom, A., Solórzano Kraemer, M.M., Gabbott, S.E., 2017. The chemistry of American and African amber, copal, and resin from the genus Hymenaea. Org. Geochem. 113, 43–54.

Michener, C.D., 1954. Bees of Panamá. Bull. Am. Mus. Nat. Hist. 104, 1–176.

Mills, J., White, R., 2015. Organic Chemistry of Museum Objects, second ed. Routledge, p. 222.

Nogueira, R.T., Shepherd, G.J., Laverde Jr., A., Marsaioli, A.J., Imamura, P.M., 2001. Clerodane-type diterpenes from the seed pods of *Hymenaea courbaril* var. *stilbocarpa*. Phytochem 58, 1153–1157.

Nogueira-Neto, P., 1997. Vida e criação de abelhas indígenas sem ferrão. Editora Nogueirapis, São Paulo.

Pennacchio, M., Jefferson, L., Havens, K., 2010. Uses and Abuses of Plant-Derived Smoke: its Ethnobotany as Hallucinogen, Perfume, Incense, and Medicine. Oxford University Press.

Pinto, A.C., Braga, W.F., Rezende, C.M., Garrido, F.M.S., Veiga, V.F., Bergter, L., Patitucci, M.L., Antunes, O.A.C., 2000. Separation of acid diterpenes of *Copaifera cearensis* Huber ex Ducke by flash chromatography using potassium hydroxide impregnated silica gel. J. Braz. Chem. Soc. 11, 355–360. https://doi.org/10.1590/S0103-50532000000400005.

Quezada-Euán, J.J.G., Nates-Parra, G., Maués, M.M., Roubik, D.W., Imperatriz-Fonseca, V.L., 2018. The economic and cultural values of stingless bees (Hymenoptera: Meliponini) among ethnic groups of tropical America. Sociobiology 65 (4), 534–557.

Ragazzi, E., Roghi, G., Giaretta, A., Gianolla, P., 2003. Classification of amber based on thermal analysis. Thermochim. Acta 404 (1–2), 43–54.

Regert, M., Colinart, S., Degrand, L., Decavallas, O., 2001. Chemical alteration and use of beeswax through time: accelerated ageing tests and analysis of archaeological samples from various environmental contexts. Archaeometry 43, 549–569.

Ruddle, K., 1973. The human use of insects: examples from the Yukpa. Biotropica 5, 94–101.

Schrader, B., 1995. Infrared and Raman Spectroscopy. Methods and Applications. VCH Verlagsgesellschaft mbH, Weinheim, Germany, p. 801.

Seyfullah, L.J., Sadowski, E.-M., Schmidt, A.R., 2015. Species-level determination of closely related araucarian resins using FTIR spectroscopy and its implications for the provenance of New Zealand amber. PeerJ 3, e1067.

Shedrinsky, A.M., Wampler, T.P., Indictor, N., Baer, N., 1989. Application of analytical pyrolysis to problems in art and archaeology: a review. J. Anal. Appl. Pyrol. 15, 393–412. https://doi.org/10.1016/0165-2370(89)85050-8.

Shillito, L.-M., Almond, M., Wicks, K., Marshall, L.-J.R., Matthews, W., 2008. The use of FT-IR as a screening technique for organic residue analysis of archaeological samples. Spectrochim. Acta A 72, 120–125. https://doi.org/10.1016/j.saa.2008.08.016.

Solórzano Kraemer, M.M., Delclòs, X., Clapham, M.E., Arillo, A., Peris, D., Jäger, P., Stebner, F., Peñalver, E., 2018. Arthropods in modern resins reveal if amber accurately recorded forest arthropod communities. Proc. Natl. Acad. Sci. 115 (26), 6739–6744.

Stankiewicz, B.A., Poinar, H.N., Briggs, D.E.G., Evershed, R.P., Poinar, G.O., 1998. Chemical preservation of plants and insects in natural resins. P. R. Soc. B 265, 1397. https://doi.org/10.1098/rspb.1998.0342.

Stearman, A.M., 1989. Yuquí: Forest Nomads in a Changing World. Holt, Rinehart and Winston, Fort Worth.

Stearman, A.M., Stierlin, E., Sigman, M.E., Roubik, D.W., Dorrien, D., 2008. Stradivarius in the jungle: traditional knowledge and the use of "black beeswax" among the Yuquí of the Bolivian Amazon. Hum. Ecol. 36, 149–159.

Stone, D., 1963. Cult traits in southeastern Costa Rica and their significance. Am. Antiq. 28, 339–359.

Swain, F.M., 1970. Non-Marine Organic Geochemistry. Cambridge University Press, p. 168.

Tappert, R., Wolfe, A.P., McKellar, R.C., Tappert, M.C., Muehlenbachs, K., 2011. Characterizing modern and fossil gymnosperm exudates using micro-Fourier transform infrared spectroscopy. Int. J. Plant Sci. 172, 120–138.

Traoré, M., Kaal, J., Martínez Cortizas, A., 2018. Chemometric tools for identification of wood from different oak species and their potential for provenancing of Iberian shipwrecks (16th-18th centuries AD). J. Archaeol. Sci. 100, 62–73.

Van den Berg, K.J., 2003. MOLART Report 10, Analysis of Diterpenoid Resins and Polymers in Paint Media and Varnishes (With an Atlas of Mass Spectra). FOM Institute AMOLF Amsterdam, p. 128 available at: http://wiki.collectiewijzer.nl/images/8/84/Molart_Report_10.pdf.

Velásquez-Runk, J., 2009. Social and river networks for the trees: wounaan's riverine rhizomic cosmos and arboreal conservation. Am. Anthropol. 111 (4), 456–467. https://doi.org/10.1111/j.1548-1433.2009.01155.x.

Verril, H.A., 1972. A mystery of the vanished past in Panama: newly discovered relics of a vanished civilization destroyed by earthquake or volcanic eruption. Illus. Lond. News 173, 15–18.

Victoria-Lona, N.V., 2012. Objects made of copal resin: a radiological analysis. Bol. Soc. Geol. Mex. 64 (2), 207–213.

Wagner-Wysiecka, E., 2018. Mid-infrared spectroscopy for characterization of Baltic amber (succinite). Spectrochim. Acta A 196, 418–431.

Wenig, P., 2011. Post-optimization of Py-GC/MS data: a case study using a new digital chemical noise reduction filter (NOISERA) to enhance the data quality utilizing OpenChrom mass spectrometric software. J. Anal. Appl. Pyrol. 92, 202–208.

Wenig, P., Odermatt, J., 2010. Efficient analysis of Py-GC/MS data by a large scale automatic database approach: an illustration of white pitch identification in pulp and paper industry. J. Anal. Appl. Pyrol. 87, 85–92.

Wenig, P., Odermatt, J., 2010. OpenChrom: a cross-platform open source software for the mass spectrometric analysis of chromatographic data. BMC Bioinf. 11, 405.

Zegouagh, Y., Derenne, S., Dignac, M.-F., Baruiso, E., Mariotti, A., Largeau, C., 2004. Demineralisation of a crop soil by mild hydrofluoric acid treatment. Influence on organic matter composition and pyrolysis. J. Anal. Appl. Pyrol. 71, 119–135.

Zelsman, J., 1959. A Río Grande burial. Panama Archaeol. 2, 85–90.

Łucejko, J., Connan, J., Orsini, S., Ribechini, E., Modugno, F., 2017. Chemical analyses of Egyptian mummification balms and organic residues from storage jars dated from the Old Kingdom to the Copto-Byzantine period. J. Archaeol. Sci. 85, 1–12.